

# Docosahexaenoic acid protection against palmitic acid-induced lipotoxicity in NGF-differentiated PC12 cells involves enhancement of autophagy and inhibition of apoptosis and necroptosis

Manuel L. Montero | Jo-Wen Liu | José Orozco | Carlos A. Casiano |  
Marino De Leon 

Center for Health Disparities and Molecular Medicine and Department of Basic Sciences, Loma Linda University School of Medicine, Loma Linda, CA, USA

## Correspondence

Marino De Leon, Center for Health Disparities and Molecular Medicine, Loma Linda University School of Medicine, Mortensen Hall 142, 11085 Campus St., Loma Linda, CA 92350, USA.  
Email: mdeleon@llu.edu

## Funding information

National Center on Minority Health and Health Disparities, Grant/Award Number: P20MD006988; National Institute of General Medical Sciences, Grant/Award Number: R25GM060507

## Abstract

Lipotoxicity (LTx) leads to cellular dysfunction and cell death and has been proposed to be an underlying process during traumatic and hypoxic injuries and neurodegenerative conditions in the nervous system. This study examines cellular mechanisms responsible for docosahexaenoic acid (DHA 22:6 n-3) protection in nerve growth factor-differentiated pheochromocytoma (NGFDPC12) cells from palmitic acid (PAM)-mediated lipotoxicity (PAM-LTx). NGFDPC12 cells exposed to PAM show a significant lipotoxicity demonstrated by a robust loss of cell viability, apoptosis, and increased HIF-1 $\alpha$  and BCL2/adenovirus E1B 19 kDa protein-interacting protein 3 gene expression. Treatment of NGFDPC12 cells undergoing PAM-LTx with the pan-caspase inhibitor ZVAD did not protect, but shifted the process from apoptosis to necroptosis. This shift in cell death mechanism was evident by the appearance of the signature necroptotic Topo I protein cleavage fragments, phosphorylation of mixed lineage kinase domain-like, and inhibition with necrostatin-1. Cultures exposed to PAM and co-treated with necrostatin-1 (necroptosis inhibitor) and rapamycin (autophagy promoter), showed a significant protection against PAM-LTx compared to necrostatin-1 alone. In addition, co-treatment with DHA, as well as 20:5 n-3, 20:4 n-6, and 22:5 n-3, in the presence of PAM protected NGFDPC12 cells against LTx. DHA-induced neuroprotection includes restoring normal levels of HIF-1 $\alpha$  and BCL2/adenovirus E1B 19 kDa protein-interacting protein 3 transcripts and caspase 8 and caspase 3 activity, phosphorylation of beclin-1, de-phosphorylation of mixed lineage kinase domain-like, increase in LC3-II, and up-regulation of Atg7 and Atg12 genes, suggesting activation of autophagy and inhibition

**Abbreviations:** ARA, arachidonic acid 20:4 n-6; Atg12, autophagy-related gene 12; Atg7, autophagy-related gene 7; BNIP3, BCL2/adenovirus E1B 19 kDa protein-interacting protein 3; CQ, chloroquine; DCF, 2'7' dichlorodihydrofluorescein diacetate; DHA, docosahexaenoic acid 22:6 n-3; n-3 DPA, n-3 docosapentaenoic acid 22:5 n-3; n-6 DPA, n-6 docosapentaenoic acid 22:5 n-6; EPA, eicosapentaenoic acid 20:5 n-3; FFA, free fatty acid; HIF-1 $\alpha$ , hypoxia-inducible factor-1 alpha; LC3 I, microtubule-associated protein 1 light chain I; LC3 II, microtubule-associated protein 1 light chain II; MLKL, mixed lineage kinase domain-like; Nec-1, necrostatin-1; NGF, nerve growth factor; NGFDPC12, nerve growth factor-differentiated pheochromocytoma cell line 12; PAM-LTx, palmitic acid-induced lipotoxicity; PUFA, polyunsaturated fatty acid; RIP3, receptor interacting protein 3; ROS, reactive oxygen species; Stau, staurosporine; Topo I, topoisomerase I; ZVAD, carbobenzoxy-valyl-alanyl-aspartyl-[O-methyl] fluoromethylketone.

This is an open access article under the terms of the Creative Commons Attribution-NonCommercial License, which permits use, distribution and reproduction in any medium, provided the original work is properly cited and is not used for commercial purposes.

© 2020 The Authors. *Journal of Neurochemistry* published by John Wiley & Sons Ltd on behalf of International Society for Neurochemistry

of necroptosis. Furthermore, DHA-induced protection was suppressed by the lysosomotropic agent chloroquine, an inhibitor of autophagy. We conclude that DHA elicits neuroprotection by regulating multiple cell death pathways including enhancement of autophagy and inhibiting apoptosis and necroptosis.

## 1 | INTRODUCTION

Free fatty acids (FFAs) play essential roles in membrane structure, signal transduction, and energy usage/storage. However, non-adipocytes cells exposed to saturated FFAs overload exhibit lipotoxicity (LTx) with detrimental consequences including cell death (Leroy, Tricot, Lacour, & Grynberg, 2008; Listenberger & Schaffer, 2002; Scheff & Dhillon, 2004; Ulloth, Casiano, & De Leon, 2003). Neurons are particularly at risk of saturated FFAs overload because triacylglycerols synthesis plays only a minor role in neuronal lipid metabolism (Tracey, Steyn, Wolvetang, & Ngo, 2018). This increased vulnerability can exacerbate the loss of neuronal viability during conditions leading to nervous system trauma (Dhillon, Dose, Scheff, & Prasad, 1997; Rodriguez de Turco et al., 2002). Our group and others have shown that exposure to high levels of saturated FFAs like stearic and palmitic acid (PAM), triggers apoptosis in nerve growth factor-differentiated PC12 (NGFDPC12) cells, primary rat cortical cells, Schwann cells, and microglial cells (Almaguel, Liu, Pacheco, Casiano, & De Leon, 2009; Descorbeth, Figueroa, Serrano-Illan, & De Leon, 2018; Padilla, Descorbeth, Almeyda, Payne, & De Leon, 2011; Patil & Chan, 2005; Ulloth et al., 2003; Wang et al., 2012). PAM overload triggers LTx as evidenced by increased cell death, reactive oxygen species, ER stress, and other cellular disruptions typical of lipotoxic injury (Han & Kaufman, 2016; Patil & Chan, 2005; Wang et al., 2012). Inhibition of caspase 3 with the pan-caspase inhibitor *N*-benzyloxycarbonyl-Val-Ala-Asp-[O-methyl]-fluoromethylketone (ZVAD) did not prevent either apoptosis or loss of viability of NGFDPC12 cells treated with PAM (Ulloth et al., 2003). These results suggested that cells exposed to PAM overload in the presence of ZVAD undergo caspase-independent cell death (Almaguel et al., 2009, 2010; Ulloth et al., 2003). This is consistent with studies showing that inhibition of caspase activation can result in a switch from apoptotic to necroptotic cell death (Galluzzi, Kepp, Krautwald, Kroemer, & Linkermann, 2014).

Necroptosis is driven by the kinases RIP1 and receptor-interacting proteins 1 and 3 (RIP3), which together with mixed lineage kinase domain-like (MLKL) form the necroptosome. Upon phosphorylation in the necroptosome, MLKL forms pores in the plasma membrane, triggering release of intracellular contents, and lysosomal membrane permeabilization (LMP), with ensuing cytoplasmic degradation (Holler et al., 2000; Meng et al., 2016; Su, Yang, Xie, DeWitt, & Chen, 2016). Plasma membrane permeabilization is a biochemical hallmark common to necroptosis, primary necrosis, and secondary necrosis that leads to the release of intracellular damage-associated molecular patterns (DAMPs) into the extracellular milieu, resulting in a proinflammatory immune response (Vanden Berghe et al., 2010). Under normal cell

growth conditions, apoptosis and necroptosis are under a precise interdependent control. For instance, during apoptosis, caspase 8 cleaves and inactivates RIP3, preventing activation of necroptosis, whereas lack of functional caspase 8 may lead to necroptosome activation (Feltham, Vince, & Lawlor, 2017; Newton et al., 2014). Apoptosis is the preferred mode of cell death under normal and pathological states because of its non-inflammatory properties and highly organized and efficient cell demise program. However, in recent years necroptosis has emerged as a key pro-inflammatory mode of cell death in the pathogenesis of human disease, including renal ischemic reperfusion injury, cardiac hypoxic injury, and brain injury (Linkermann et al., 2012; Northington et al., 2011; Oerlemans et al., 2012; Smith et al., 2007; Zhu, Zhang, Bai, & Li, 2011). Another critical cellular process is autophagy, which mediates the elimination of intracellular molecules and organelles to maintain homeostasis and survival in the presence of stress (Green & Levine, 2014; Wirawan, Vanden Berghe, Lippens, Agostinis, & Vandenabeele, 2012). This process is critical for maintaining cellular ATP and macromolecular recycling and can represent a pro-survival pathway (Bray et al., 2012; Degenhardt et al., 2006). Autophagy is regulated by ATG (autophagy-related) proteins and redistribution of LC3 (microtubule-associated protein 1 light chain 3), with the appearance of lipidated LC3, that is, LC3-II, as a biochemical hallmark. Autophagy in primary mice cortical cells correlates with recovery and cell survival after hypoxia/reoxygenation injury (Zhang et al., 2013). There is evidence supporting an interplay between autophagy, apoptosis, and necroptosis (Long & Ryan, 2012). Whether the cell survives or dies by a particular cell death modality in the presence of stress depends on the severity of cellular damage, ATP availability, and levels of endogenous inhibitors of specific survival/cell death pathways (Damme, Suintio, Saftig, & Eskelinen, 2014; Long & Ryan, 2012). Docosahexaenoic acid (DHA) is the major n-3 polyunsaturated fatty acid (PUFA) component in neuronal membranes in the gray matter of the cerebral cortex and in retinal photoreceptors cells (Lauritzen et al., 2000; Yehuda, Rabinovitz, Carasso, & Mostofsky, 2002). In previous reports we showed that DHA inhibits PAM-LTx-induced apoptosis in NGFDPC12 and Schwann cells (Almaguel et al., 2009; Descorbeth et al., 2018), protects NGFDPC12 cells against PAM-induced lysosomal and mitochondrial permeabilization (Almaguel et al., 2010), and attenuates neuronal dysfunction following experimental spinal cord injury (Figueroa et al., 2012). Furthermore, DHA-derived metabolites have been associated with anti-nociceptive responses after experimental spinal cord injury (Figueroa et al., 2012; Figueroa, Cordero, Llan, & De Leon, 2013; Figueroa, Cordero, Serrano-Illan, et al., 2013). This study examines the interactions between apoptosis, necroptosis, and autophagy in the context of DHA-induced protection of NGFDPC12 cells from PAM-LTx.



## 2 | MATERIALS AND METHODS

### 2.1 | Reagents

Reagents were purchased from the indicated suppliers as follows: Ham's F-12 medium with Kaighn's modification (F-12K) was from Mediatech, Inc.; horse serum and fetal bovine serum were from Atlantic Biological; nerve growth factor (NGF, Cat# N-100) was from Alomone Labs; fatty acid-free bovine serum albumin (Cat# 126575-10GM) was from EMD Millipore Corp; palmitic acid (PAM, Cat# P0500-25G), protease inhibitor cocktail tablets (Cat# 4693124001), and chloroquine diphosphate (Cat# C6628-25G) were from Sigma-Aldrich (St. Louis, MO); DHA (Cat# 90310), eicosapentanoic acid (EPA, Cat# 90110), arachidonic acid (ARA, Cat# 90010), n-3 docosapentanoic acid (DPA, Cat# 90165), and n-6 docosapentaenoic acid 22:5 n-6 (n-6 DPA) (Cat# 10,008,335) were from Cayman Chemicals; ZVAD (Cat# ALX-260-020-M005), staurosporine (Cat# ALX-380-014-M001), and necrostatin-1 (Cat# BML-AP309-0020) were from Enzo Life Science; mercuric chloride ( $\text{HgCl}_2$ , Cat# 201,430,250) was from Acros Organics; rapamycin (Cat# 99045) was from Cell Signaling Technology.

### 2.2 | Cell culture and treatments

Rat pheochromocytoma clone 12 (PC12 cells, RRID:CVCL\_0481, ATCC Cat# CRL-1721, Manassas, VA) is not listed as a commonly misidentified cell line and was last authenticated on March 2018 by comparing DNA sequence of STR marker 18-3 with the NCBI databases. All the cells we used in this study were within seven passages. PC12 cells were cultured in F-12K medium with 15% horse serum, 2.5% fetal bovine serum (FBS), and penicillin/streptomycin. After attaching to culture plates, cells were then differentiated with F-12K medium containing NGF (50 ng/ml) and 1% FBS and penicillin/streptomycin (1% FBS-NGF medium). Medium was changed every 2–3 days and cells were differentiated for 7–10 days before experimental treatments. Fully differentiated PC12 cells showing long neurites that form an extensive network were used in all experimental conditions.

PAM-LTx treatment was performed as previously described (Almaguel et al., 2009; Ulloth et al., 2003). Briefly, a PAM stock solution (300 mM in 100% ethanol) was diluted 1,000-fold in warm 1% FBS-NGF medium containing 0.15 mM fatty acid-free bovine serum albumin (BSA) resulting in a complex of PAM:BSA at 2:1 (0.3 mM:0.15 mM) molar ratio. Previous analysis showed that PAM:BSA at 2:1 ratio results in unbound-free PAM at low nM concentration throughout the course of the experiment (Almaguel et al., 2009).

DHA and other PUFA stock (50 mM) were also prepared in 100% ethanol and diluted in 1% FBS-NGF medium containing 0.15 mM fatty acid-free BSA with or without PAM. For control, cells were treated with 1% FBS-NGF medium containing 0.15 mM fatty acid-free BSA and 0.1% ethanol. Cell morphology after treatment was documented using a phase contrast IX70 Olympus microscope equipped with a SPOT-Insight CMOS camera. The cell death modulators ZVAD, necrostatin-1, rapamycin, chloroquine, staurosporine,

and  $\text{HgCl}_2$  were added to the media at the same time with PAM treatment. ZVAD, necrostatin-1, staurosporine, and rapamycin were dissolved in DMSO.  $\text{HgCl}_2$  and chloroquine were dissolved in water. The treatment of cultures with these cell death modulators was performed without pre-treatment because PAM overload toxicity effect can be reverse within the first 4–6 hr after the initial treatment (Almaguel et al., 2009).

### 2.3 | Quantitative real-time PCR analysis

Procedures for total RNA extraction, cDNA synthesis, and quantitative RT-PCR were described previously (Almaguel et al., 2009; Padilla et al., 2011). Relative amount of mRNA was calculated by the  $2^{-\Delta\Delta\text{CT}}$  method, using  $\beta$ -actin as reference gene. The primer sets used are as following:

HIF-1 $\alpha$ : 5'-TCCATGTGACCATGAGGAAA-3' and 5'-CTTCCACGT TGCTGACTTGA-3'; BNIP3: 5'-CCAGAAAATGTTCCCCCAAG-3' and 5'-TTGTCAGACGCTTCCAATGTAG-3'; Atg7: 5'-CCCAAAGAC ATCAAGGGCTA-3' and 5'-CCTGACTTTATGGCTTCCCA-3'; Atg12: 5'-CGTCTTCGGTTGCAGTTTC-3' and 5'-CCAGTTTACCATCACTGCC A-3';  $\beta$ -actin: 5'-GGGAAATCGTGCCTGACATT-3' and 5'-GCGGCAGT GGCCATCTC-3'.

### 2.4 | Reactive oxygen species analysis

Cellular ROS levels were measured by flow cytometry using the fluorescent indicator 2',7'-dichlorodihydrofluorescein diacetate ( $\text{H}_2\text{DCFDA}$ ; Thermo Fisher Scientific). After treatment, NGFDPC12 cells were incubated with 10  $\mu\text{M}$   $\text{H}_2\text{DCFDA}$  in F-12K medium for 25 min at 37°C. Cells were then detached by HyClone HyQtase (GE Healthcare), rinsed and analyzed with a Becton-Dickinson FACSCalibur (Almaguel et al., 2009; Padilla et al., 2011). NGFDPC12 cells treated with 10  $\mu\text{M}$  DL-Buthionine-[S,R]-sulfoximine (BSO) for 24 hr served as positive control.

### 2.5 | Apoptosis detection

After treatment, NGFDPC12 cells were detached from plates by HyQtase (HyClone) and incubated with the apoptosis marker Annexin V-FITC for 20 min. Annexin V positive cells were detected by flow cytometry as described previously (Padilla et al., 2011).

### 2.6 | Caspase activity assay

The activity of caspases 3 and 8 in NGFDPC12 cells after treatment was analyzed with colorimetric assay kits from Enzo Life Sciences (Cat# ALX-850-215-K101 for caspase 3 and ALX-850-221-K101 for caspase 8). Following manufacturer's instructions, cells were extracted with lysis buffer and protein concentration in the cytosolic

extract was determined. Then, 50  $\mu$ l lysate containing 100  $\mu$ g protein was mixed with equal volume of 2X reaction buffer and 5  $\mu$ l of 4 mM substrate. After 1–2 hr incubation at 37°C, the OD at 405 nm was detected using Spectra Max i3X spectrophotometer. Caspase activity was calculated as average fold increase in the OD reading relative to that of control group, which was normalized to one.

## 2.7 | Determination of cell viability

Cell viability after PAM-LTx treatment was determined by crystal violet assay. PC12 cells were seeded in 6- or 12-well plates at a density of 7,500 cells/cm<sup>2</sup> and differentiated with NGF. After treatment, cells were gently rinsed, fixed, and stained with crystal violet solution as stated before (Padilla et al., 2011). Bound crystal violet was dissolved with 10% acetic acid and the optical density (OD) at 570 nm was determined using a Spectra Max i3X spectrophotometer (Molecular Devices). Cell viability was calculated as average percent of the OD reading relative to that of control group, which was normalized to 100%.

## 2.8 | Antibodies and immunoblotting

DNA topoisomerase I (Topo I) and its cell death-associated cleavage fragments were detected by immunoblotting using human scleroderma-associated autoantibodies (dilution 1:200) as described previously (Pacheco, Almaguel, & Evans, 2014; Pacheco et al., 2005). LC3 (Cat# 4108S, dilution 1:2,500), phospho-beclin-1 (Ser93, Cat# 14717S, dilution 1:2,000), and beclin-1 (Cat# 3495SRRID; AB\_1903911, dilution 1:1,000) antibodies were purchased from Cell Signaling Technology. Phospho-MLKL antibody (Cat# ab196436, dilution 1:1,000) was from Abcam and  $\beta$ -actin antibody was from Sigma-Aldrich (Cat# A5441-0.2MI, dilution 1:5,000). We used Laemmli Sample Buffer (0.1 M Tris-HCl, pH 6.8 containing 4% SDS, 10% glycerol, and protease inhibitors) to extract total protein from cells. After quantification, 15–40  $\mu$ g of cellular proteins was resolved on a 4%–12% NuPAGE Bis-Tris Gel (Invitrogen) and transferred to nitrocellulose membranes. Membranes were blocked with Odyssey blocking buffer (Cat# 927-50000; Li-Cor Biotechnology) and incubated with primary antibodies overnight at 4°C. After washes, the membranes were incubated with IRDye secondary antibodies (IRDye 680RD goat anti-rabbit IgG 926-68071, RRID:AB\_10956166, and IRDye 800CW goat anti-mouse 926-32210, RRID:AB\_621842; Li-Cor Biotechnology) at 1:30,000 dilution for subsequent Odyssey imaging (Li-Cor Biotechnology). Quantitative analysis was done within the dynamic range of the equipment. Because of lack of proper IRDye secondary antibody, Topo I immunoblots were incubated with HRP-conjugated anti-human secondary antibody (dilution 1:5,000, Cat# A18847, RRID:AB\_2535624; Thermo Fisher Scientific) and anti-mouse secondary antibody (dilution 1:10,000, Cat# G-21040, RRID:AB\_2536527; Thermo Fisher Scientific) followed by chemiluminescent detection. All signals are within the linear range of the gray scale.

## 2.9 | Study design and statistical analysis

This study was not pre-registered and no randomization or blinding was performed. No sample size calculation was used to predetermine the sample size in this study. All measurements were done in triplicates in at least three independent cell cultures. Data analysis was done by GraphPad Prism 6.0 (GraphPad Software). Identification of outliers was done with ROUT ( $Q = 5\%$ ) and normality of data was assessed with Kolmogorov–Smirnov test. Statistical comparison analysis for multi-group experiments was performed by either one-way ANOVA or two-way ANOVA followed by multiple comparison test. Experiments comparing two groups were analyzed by Student's *t* test. Significance was accepted at  $p < .05$ .

## 3 | RESULTS

### 3.1 | PAM-LTx involves a stress cellular response and apoptosis in NGFDPC12 cells

PAM overload stimulates cellular ROS generation (Almaguel et al., 2009; Liu, Montero, Bu, & De Leon, 2015), which in turn activates cellular stress response proteins, including hypoxia-inducible factor 1 (HIF-1 $\alpha$ ). Figure 1a shows a time course of HIF-1 $\alpha$  mRNA expression following PAM overload. Notice a significant increase in HIF-1 $\alpha$  expression at 24 (3.7-fold) and 48 (3.8-fold) hours after treatment. One of the downstream effects of HIF-1 $\alpha$  is up-regulation of the pro-apoptotic gene BNIP3 (BCL2/adenovirus E1B 19 kDa protein-interacting protein 3) (Guo, 2017). Figure 1b demonstrates an increase in BNIP3 mRNA levels at 18 (3.5-fold), 24 (3.3-fold), and 48 hr (3.9-fold) after PAM treatment, which is consistent with our previous report showing that PAM induces apoptosis in NGFDPC12 cells (Almaguel et al., 2009). Next, we confirmed that PAM overload triggers significant early apoptosis in our experimental conditions, by incubating cells with Annexin V after treatment. Figure 1c shows a 3-fold increase in apoptotic cells after a 24 hr exposure to PAM compared to control.

### 3.2 | ZVAD drives PAM-LTx-induced NGFDPC12 cell necroptosis

In a previous study, our group showed that PAM-LTx overload induces loss of NGFDPC12 cell viability through apoptosis; however, the pan-caspase inhibitor ZVAD did not protect against this stressor since cells were still capable of dying by a caspase-independent cell death process (Ulloa et al., 2003). In the next series of experiments, we examined if caspase-independent cell death following exposure to PAM + ZVAD is necroptotic. For these experiments we used a highly specific human autoantibody to nuclear protein Topoisomerase I (Topo I) that discriminates between apoptosis and necrosis (primary, secondary, and necroptosis) in immunoblots of protein lysates from affected cells (Casiano, Martin, Green,

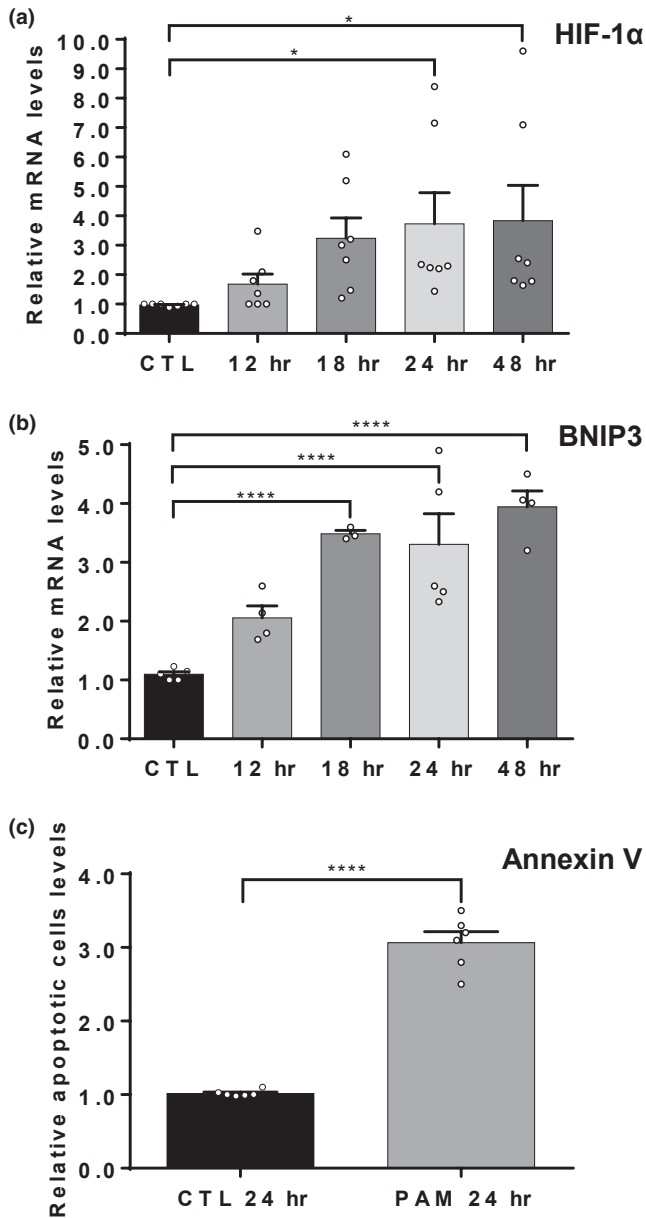


**FIGURE 1** Palmitic acid-induced lipotoxicity (PAM-LTx) stimulates HIF-1 $\alpha$  and BNIP3 mRNA expression and apoptosis in NGFDPC12 cells. NGFDPC12 cells were treated with BSA control medium (CTL) or PAM complexed with fatty acid-free BSA at 2:1 ratio (PAM) for 12, 18, 24, and 48 hr and the levels of (a) HIF-1 $\alpha$  and (b) BNIP3 mRNA were analyzed by real-time RT-PCR. (c) NGFDPC12 cells were treated with PAM for 24 hr and apoptotic cells were identified by Annexin V labeling. The percentage of Annexin V-tagged cells in a sample was determined by flow cytometry. The results are expressed as fold-change relative to control at 24 hr and the data are shown as mean  $\pm$  SEM,  $n = 7$  (a),  $n = 3-5$  (b), and  $n = 6$  (c) of independent cell culture preparations. Statistical analysis was done by one-way ANOVA followed by multiple comparison test for (a) and (b) and by Student's *t* test for (c). Significance symbols: \* $p < .05$ ; \*\*\*\* $p < .0001$

& Tan, 1996; Casiano, Ochs, & Tan, 1998; Pacheco et al., 2005, 2014; Wu, Molinaro, Johnson, & Casiano, 2001). This autoantibody was shown to specifically recognize Topo I 70 and 45 kDa cleavage

fragments generated during necrosis or necroptosis; and a single Topo I 70 kDa cleavage signature of apoptosis (Casiano et al., 1996, 1998; Pacheco et al., 2005) (Pacheco et al., 2014; Wu et al., 2001). In order to validate these published observations in our system, we performed a series of immunoblots using cell lysates of NGFDPC12 cell cultures treated with staurosporine and HgCl<sub>2</sub>, two well-established inducers of apoptosis and necrosis, respectively. We predicted that NGFDPC12 cells should present the same cleavage pattern of Topo I during necrosis or necroptosis because primary necrosis, secondary necrosis, and necroptosis converge into downstream cathepsin-mediated proteolysis, and exhibit identical patterns of Topo I cleavage in L929 fibroblasts (Pacheco et al., 2005, 2014). ZVAD has been shown to stimulate necroptosis in cells exposed to high level of stress (Long & Ryan, 2012). Thus we predicted that cultures exposed to PAM would generate a necroptotic Topo 1 pattern. As predicted, Figure 2a shows the apoptotic 70 kDa fragment after treatment with the apoptosis inducer staurosporine (Stau lanes). The faint 45 kDa band in staurosporine-treated samples was likely because of basal secondary necrosis (Silva, 2010; Wu et al., 2001). HgCl<sub>2</sub> induced the signature necrosis-associated Topo I cleavage pattern (70 and 45 kDa fragments) at 6, 12, 18, and 24 hr (Figure 2a and 2b). The 60 kDa band shown in all treatment groups in Figure 2a was likely because of non-specific autoantibody binding. Next, the induction of apoptosis in NGFDPC12 cells treated with PAM was confirmed by the appearance of the 70 kDa apoptotic cleavage fragment of Topo I, without the presence of the necrotic 45 kDa fragment (Figure 2b, PAM 24 and 48 hr lanes). In contrast, when the pan-caspase inhibitor ZVAD was added to cultures exposed to PAM, we observed the necrosis-associated 45 kDa cleavage fragment (Figure 2b, PAM + ZVAD 24 and 48 hr-lanes). Notice the reduction in the 70 kDa fragment after 48 hr of PAM treatment suggesting the activation of secondary necrosis considering the low energy available at that time point and the high energy demand of the apoptotic process required for the formation of the apoptosome and caspase activation (Leist, Single, Castoldi, Kuhnle, & Nicotera, 1997). Caspases will digest Topoisomerase I as long as there is ATP available. In our system, there is mitochondrial dysfunction as early as 12 hr (Almaguel et al., 2010) which may affect production of ATP and thus resulting in secondary necrosis by 48 hr (Eguchi, Shimizu, & Tsujimoto, 1997; Salvesen & Renshaw, 2002). In contrast, the PAM + ZVAD condition shows only a small reduction in the 45kDa Topo 1 cleavage mostly because of the capacity of cathepsins to function even at low ATP levels (Sato et al., 2008). Furthermore, some of the Topo I protein may have been digested even further into lower size products by cathepsins or released from the small blebs into the medium during the process of secondary necrosis. In contrast, cultures of cells undergoing primary necrosis or necroptosis (i.e. PAM + ZVAD) yield a higher protein content because, in spite of their membrane permeabilization, cells have not been previously fragmented into multiple small blebs that are difficult to collect for lysate preparation. These findings indicated that ZVAD drives PAM-LTx overload toward necroptosis.

In order to further test the hypothesis that necroptosis was driven by ZVAD during PAM treatment in NGFDPC12 cultures, we

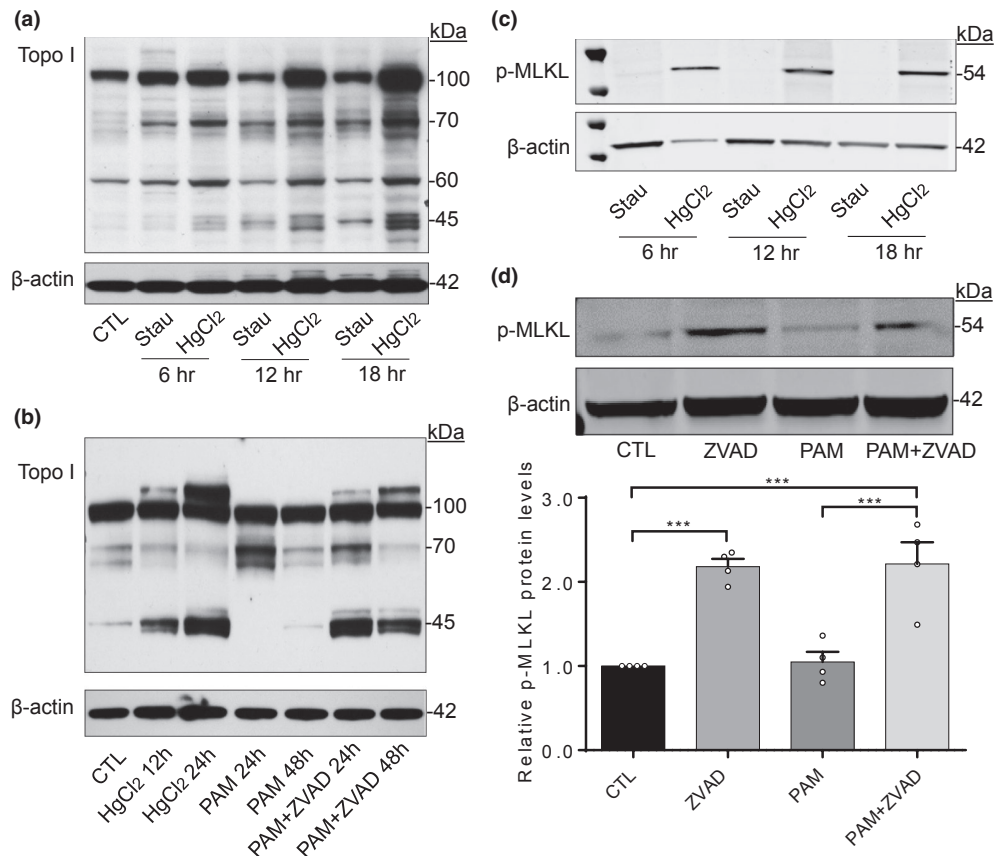


**FIGURE 2** Cleavage pattern of Topo I and Phosphorylation of MLKL in palmitic acid (PAM)- treated NGFDPC12 cells in the presence or absence of ZVAD. (a) The cleavage pattern of Topo I has been shown to differentiate between apoptosis and either necrosis or necroptosis. For validation of using this method in NGFDPC12 cells, we treated cells with BSA control medium (CTL), the established apoptosis inducer staurosporine (Stau, 3 $\mu$ M) or the necrosis inducer HgCl<sub>2</sub> (50  $\mu$ M) for 6, 12, and 18 hr. Total cellular protein was extracted and Topo I immunoblot was performed using a human autoimmune serum containing Topo I autoantibodies (1:250 dilution). (b) NGFDPC12 cells were treated with CTL and PAM in the presence or absence of ZVAD (40 $\mu$ M) for 24 and 48 hr. Cellular proteins were collected followed by Topo I immunoblotting. (c) To clarify whether HgCl<sub>2</sub> was inducing markers of necroptosis we proceeded to probe the phosphorylation of MLKL. Using again staurosporine (3 $\mu$ M) and HgCl<sub>2</sub> (50 $\mu$ M) we treated the cells for 6, 12, and 18 hr. (d) NGFDPC12 cells were treated with CTL and PAM in the presence or absence of ZVAD (40  $\mu$ M). Total cellular protein was extracted after 20 hr treatment followed by p-MLKL immunoblotting. Quantification was done with Image Studio Software and p-MLKL protein level was calculated relative to its  $\beta$ -actin band. The bar graph represents the mean  $\pm$  SD,  $n = 4$  of independent cell culture preparations. Statistical analysis was done by one-way ANOVA followed by multiple comparison test. Significance symbols: \*\*\* $p < .001$

determined by immunoblotting if MLKL was phosphorylated, a hallmark of its activation during necroptotic cell death (McNamara *et al.* 2018). NGFDPC12 cells were treated with staurosporine and HgCl<sub>2</sub> and the cell lysates were used to conduct immunoblotting with an antibody that recognizes MLKL phosphoserine 345. Figure 2c shows that the specific 54 kDa band of phosphorylated MLKL is generated in HgCl<sub>2</sub> treated NGFDPC12 cells at all three time points, but it was absent in staurosporine treated cells, suggesting that HgCl<sub>2</sub> also induces necroptosis in these cells. Next, we determined if NGFDPC12 cells treated with PAM in the presence of ZVAD underwent necroptosis, as determined by the appearance of phosphorylated MLKL. Figure 2d shows a strong 54 kDa band corresponding to phosphorylated MLKL after 20 hr of treatment with ZVAD alone, which is known to induce necroptosis by itself (Khan, Lawlor, Murphy, & Vince, 2014; Zhou & Yuan, 2014). BSA control (CTL) and PAM lysates show a faint band at 54 kDa, probably because of MLKL activation

in a subset of cells undergoing necroptosis. PAM + ZVAD treatment also induced MLKL phosphorylation (Figure 2d). Note that the extent of MLKL phosphorylation in cells treated with ZVAD alone and cells treated with PAM + ZVAD was similar, suggesting that ZVAD was driving the necroptosis process. Together with the generation of the necroptotic Topo I 45kDa cleavage fragment during PAM + ZVAD treatment (Figure 2b), these results suggested that cells treated with PAM in the presence of ZVAD switched from apoptosis to necroptosis because of global caspase inhibition.

### 3.3 | Crosstalk between apoptosis and necroptosis in NGFDPC12 cells undergoing PAM-LTx

Lipotoxicity is a major cellular stressor and further attempt to inhibit this process may require targeting multiple cell death modalities and



identify potential areas of crosstalk between them. Thus, the next series of experiments used ZVAD to inhibit apoptosis, the RIP1 inhibitor necrostatin-1 (Nec-1) to inhibit necroptosis, and the mTOR inhibitor rapamycin (Rapa) to promote autophagy. NGFDPC12 cells were treated with ZVAD, Nec-1 or Rapa for 48 hr in the presence or absence of PAM (Figure 3a–c). NGFDPC12 cells treated with ZVAD alone showed a significant 20% reduction in cell viability compared to control untreated cells (Figure 3a), consistent with our observation that ZVAD by itself induces necroptotic MLKL phosphorylation (Figure 2d). PAM treatment decreased the cell viability to 35%, and, as expected, treatment with ZVAD alone did not rescue the cells from apoptosis, consistent with a complete switch to necroptosis by the combined PAM + ZVAD treatment (Figure 3a). Treatment with Nec-1 did not affect cell viability by itself but increased cell viability of PAM-treated cells (Figure 3b). The autophagy promoter rapamycin (Rapa) neither affected cell viability nor protected cells during co-treatment with PAM (Figure 3c). Thus, inhibiting apoptosis with ZVAD or stimulating autophagy alone were not sufficient to rescue

NGFDPC12 cells from PAM-LTx. Notice, however, that Nec-1 treatment had a modest protective effect against PAM-LTx overload.

The next series of experiments explored the combinatorial effect of these inhibitors and inducers on PAM-LTx overload of NGFDPC12 cells (Figure 3d–f). The combined treatment of ZVAD + Nec-1 in the absence of PAM increased cell viability by 24% compared to the untreated control cells, suggesting that this treatment may inhibit ongoing spontaneous cell death in culture (Figure 3d). PAM treatment decreased cell viability to 37%, but the combined treatment of ZVAD + Nec-1 increased it to 66% (Figure 3d). These results are consistent with the notion that inhibiting necroptosis, but not apoptosis, attenuates PAM-LTx in NGFDPC12 cells. Next, we examined the effects of inhibiting necroptosis while promoting of autophagy. The combined treatment of Nec-1 + Rapa induced a more robust effect on cell viability than that observed with ZVAD + Nec-1 (Figure 3e), and significantly increased cell viability in the absence of PAM (60% above control). In the presence of PAM, the Nec-1 + Rapa combination also significantly increased cell viability

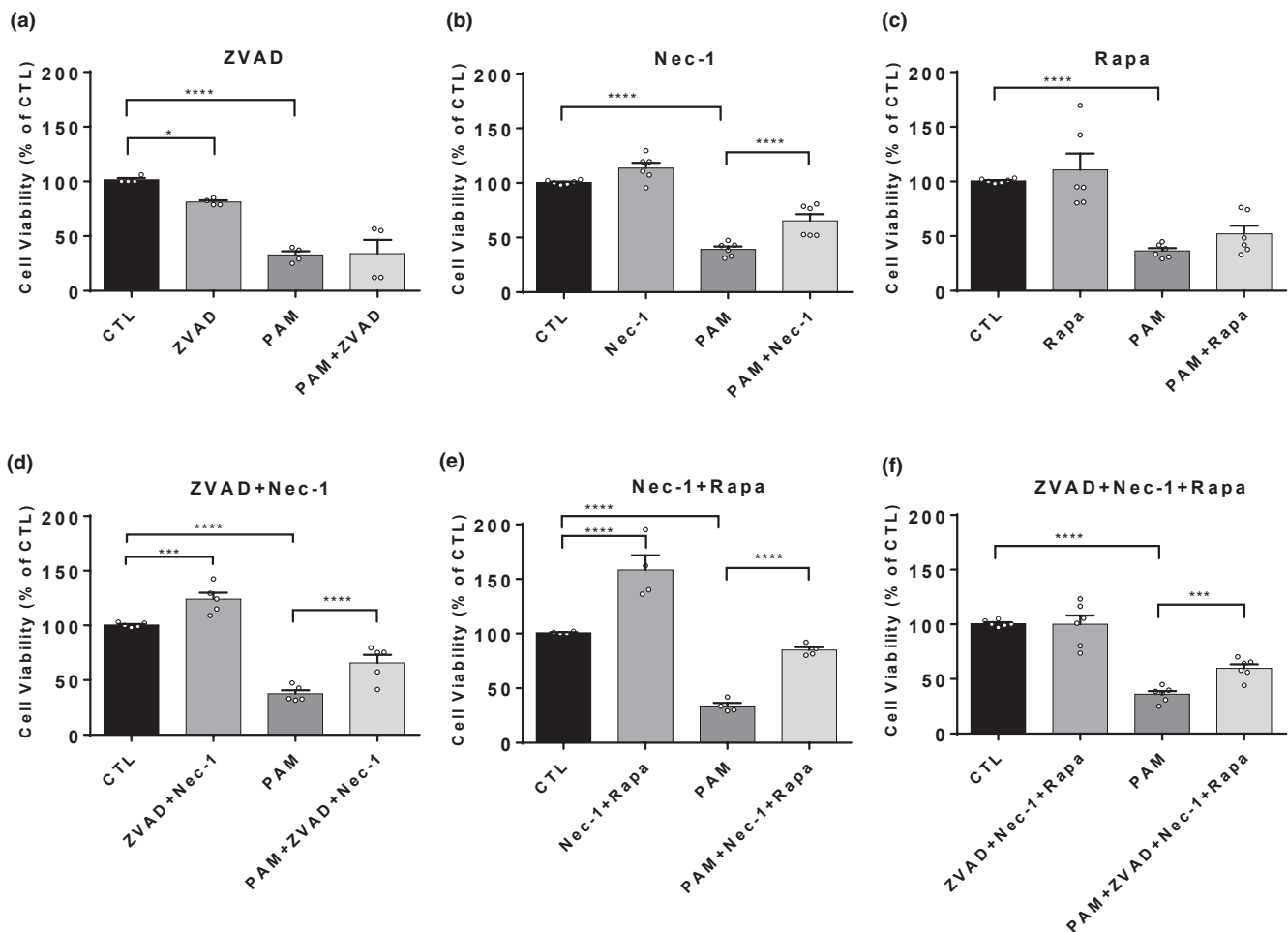


**FIGURE 3** Effects of apoptosis and necroptosis inhibitors and autophagy inducer on NGFDPC12 cells with or without palmitic acid-induced lipotoxicity (PAM-LTx). NGFDPC12 cells were treated with ZVAD at 40  $\mu$ M (a), necrostatin 1 (Nec-1) at 50  $\mu$ M (b), rapamycin (Rapa) at 100 nM (c), ZVAD + Nec-1 (d), Nec-1 + Rapa (e), and ZVAD + Nec-1 + Rapa (f) in the presence or absence of PAM-LTx. Cell viability was determined at 48 hr after treatment using crystal violet assay. The results are expressed as percent of control and the data are shown as Mean  $\pm$  SEM,  $n = 4$  (a, e), and  $n = 6$  (b–d, f) of independent cell culture preparations. Statistical analysis was done by one-way ANOVA followed by multiple comparison test. Significance symbols: \* $p < .05$ ; \*\*\* $p < .001$ ; \*\*\*\* $p < .0001$

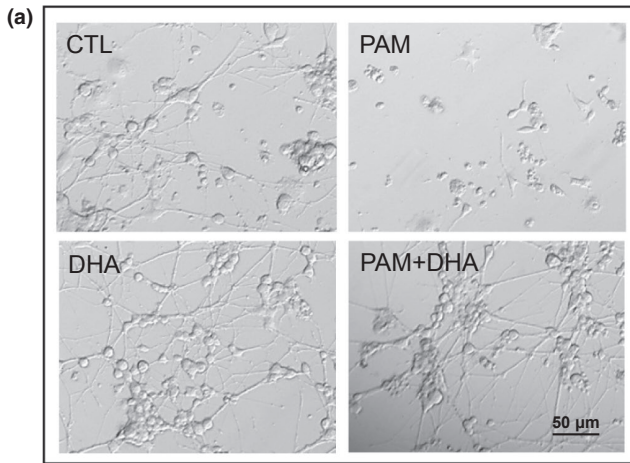
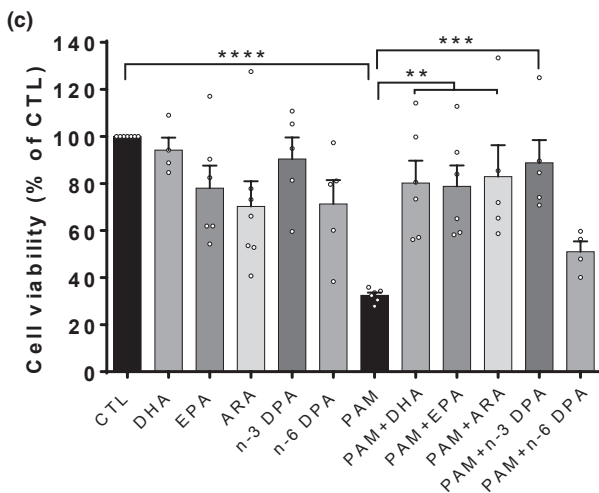
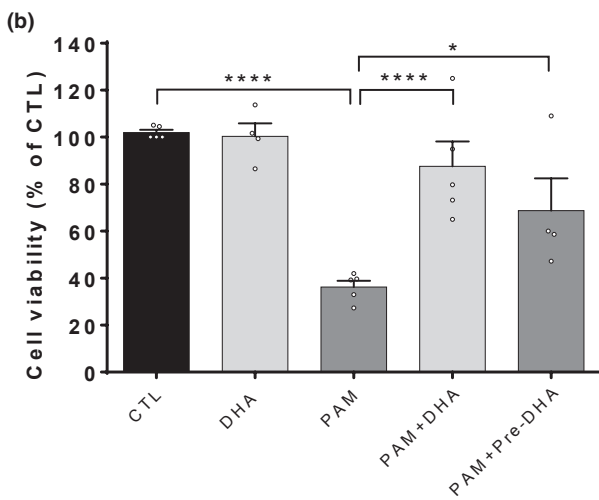


**FIGURE 4** Docosahexaenoic acid 22:6 n-3 (DHA) and related polyunsaturated fatty acids rescue NGFDPC12 cells from palmitic acid-induced lipotoxicity (PAM-LTx). (a) Microscopic images show NGFDPC12 cells 48 hr after treatment with BSA control medium (CTL), DHA (50  $\mu$ M), PAM, and PAM + DHA. (b) NGFDPC12 cells were treated as in (a) and cell viability was determined by crystal violet assay at 48 hr. For the pre-treatment group NGFDPC12 cells were treated with 50  $\mu$ M of DHA (50  $\mu$ M) for 24 hr followed by PAM-LTx without DHA for another 48 hr. (c) NGFDPC12 cells were treated with 50  $\mu$ M of DHA, eicosapentaenoic acid 20:5 n-3 (EPA), arachidonic acid 20:4 n-6, n-3 DPA, and n-6 docosapentaenoic acid 22:5 n-6 (n-6 DPA) alone or together with PAM for 48 hr and cell viability was determined by crystal violet assay. The results are expressed as percent of control and shown as Mean  $\pm$  SEM,  $n = 4-5$  (b), and  $n = 4-7$  (c) of independent cell culture preparations. Statistical analysis was done by one-way ANOVA followed by multiple comparison test. Significance symbols: \* $p < .05$ ; \*\* $p < .01$ ; \*\*\* $p < .001$ ; \*\*\*\* $p < .0001$



(84% compared to control). These results suggest that nearly full neuroprotection can be achieved if necroptosis is inhibited while autophagy is promoted. Co-treatment of cultures exposed to PAM with ZVAD + Nec-1 + Rapa also showed a significant protection (61% compared to control) (Figure 3f). Interestingly, treatment with Nec-1 and Rapa appeared to partially reverse ZVAD-induced necroptosis (Figure 3f compared to Figure 3a). Taken together, these

findings point to a dynamic interaction between autophagy and necroptosis in which the protective effects of autophagy against PAM-LTx seem to be enhanced under inhibition of necroptosis.

### 3.4 | Modulation of PAM-LTx by DHA and other PUFAs

In subsequent experiments we assessed the effects of DHA bound to fatty acid-free BSA (see Methods) on rescuing NGFDPC12 cells from PAM-LTx. Figure 4a shows that NGFDPC12 cells treated with PAM for 24 hr show abnormal morphology with small/short neurites, but display normal features when co-treated with DHA. Quantification of cell viability showed that treatment with DHA alone did not affect cell viability, but rescued NGFDPC12 cells from PAM-LTx when used in co-treatment with PAM (Figure 4b). Interestingly, a similar protective effect was also observed when cells were pre-treated with DHA before treatment with PAM (Figure 4b). We then compared the protective effects of DHA against PAM-LTx to those of polyunsaturated free fatty acids (PUFAs) with different chain length or level of desaturation. NGFDPC12 cells were treated with EPA, ARA, n-3 docosapentaenoic acid 22:5 n-3 (n-3 DPA), and n-6 DPA in the presence or absence of PAM. Figure 4c shows that there was no significant difference in cell viability between control cells and cells treated with different PUFAs alone. However, co-treatment of PAM with each of these fatty acids, except n-6 DPA, significantly increased cell viability when compared to PAM treatment alone. These findings are consistent with the notion that the protective effect of DHA during PAM-LTx may be comparable to that of other PUFAs, and further studies are needed to determine specific downstream mechanisms.

### 3.5 | DHA inhibits apoptosis and necroptosis

We next sought to determine if the protective action of DHA during PAM-LTx involves inhibition of apoptosis and necroptosis. We

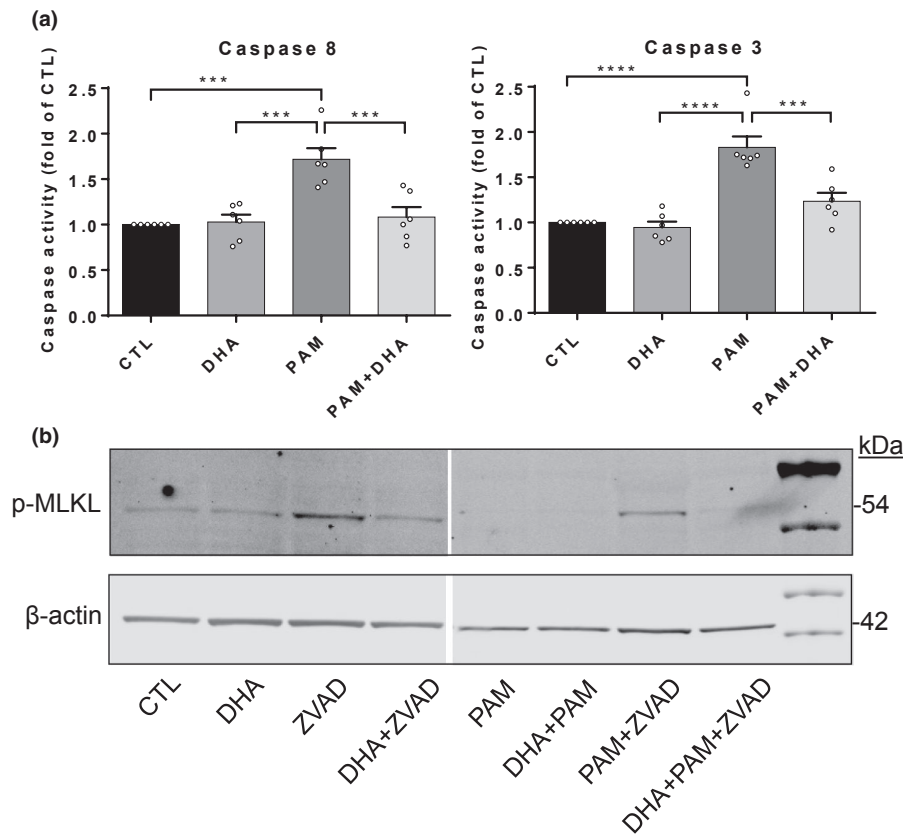


**FIGURE 5** Docosahexaenoic acid 22:6 n-3 (DHA) inhibits apoptosis and necroptosis. (a) NGFDPC12 cells were treated with BSA control medium (CTL) or palmitic acid (PAM) in the presence or absence of DHA (50 $\mu$ M). The activity of caspases 8 and 3 was probed using a colorimetric assay kit described in the Materials and Methods section. Results are expressed as fold of control and shown as Mean  $\pm$  SEM,  $n = 6$  of independent cell culture preparations. Statistical analysis was done by one-way ANOVA followed by multiple comparison test. Significance symbols: \*\*\* $p < .001$ ; \*\*\*\* $p < .0001$  (b) NGFDPC12 cells were treated with CTL, DHA, ZVAD, DHA + ZVAD with or without PAM followed with Phospho-mixed lineage kinase domain-like (p-MLKL) immunoblotting. The experiment was repeated at least three times and representative blots are shown

measured the activity of caspases 8 and 3 in NGFDPC12 cells as indicators of apoptosis after PAM overload. Caspase 8 is an initiator caspase that activates effector caspases like caspase 3 and also inhibits necroptosis and autophagy (Djavaheri-Mergny, Maiuri, & Kroemer, 2010; Luo & Rubinsztein, 2010). Figure 5a shows that DHA did not increase the activity of caspase 8 and caspase 3. PAM, on the other hand, induced a 1.7-fold increase in caspase 8 activity and 1.8-fold increase in caspase 3 activity, supporting our previous findings (Ulloa et al., 2003). However, co-treatment of DHA and PAM decreased both caspase 8 and caspase 3 activation to control levels (Figure 5a). We then examined MLKL phosphorylation to determine whether DHA rescues necroptosis induced by ZVAD in the presence of PAM. Figure 5b shows that after 20 hr of treatment, the amount of phosphorylated MLKL in NGFDPC12 cells treated with BSA-control (CTL) and DHA alone were low. These faint p-MLKL bands were often observed in our control NGFDPC12 cell cultures and probably resulted from spontaneously occurring apoptotic cells in culture which, upon transitioning to secondary necrosis, release toxic intracellular contents that induce necroptosis in nearby cells. As expected, the p-MLKL band was highly induced in the ZVAD-treated group, consistent with our previous results indicating that ZVAD

modestly induces necroptosis by itself (Figure 5b). Interestingly, addition of DHA to ZVAD-treated NGFDPC12 cells reduced the p-MLKL protein to control levels. Next, we analyzed p-MLKL levels in the context of PAM-LTx, and observed that at the same time point, treatment with PAM did not induce MLKL phosphorylation (presumably because the cells were driven into apoptosis), and co-treatment of DHA with PAM did not change the status of MLKL (Figure 5b). The appearance of phosphorylated MLKL during co-treatment with PAM and ZVAD, indicative of the switch from apoptosis to necroptosis, was completely abolished by DHA (Figure 5b). Taken together, these results are consistent with a neuroprotective role for DHA in rescuing NGFDPC12 cells from PAM-induced apoptosis, and ZVAD- or ZVAD + PAM-induced necroptosis.

### 3.6 | DHA diminishes PAM-LTx-induced HIF-1 $\alpha$ and BNIP3 but not ROS

In the next series of experiments, we quantified the expression of HIF-1 $\alpha$  and BNIP3 during PAM-LTx, in the presence or absence of DHA. DHA alone did not alter HIF-1 $\alpha$  and BNIP3 mRNA levels;

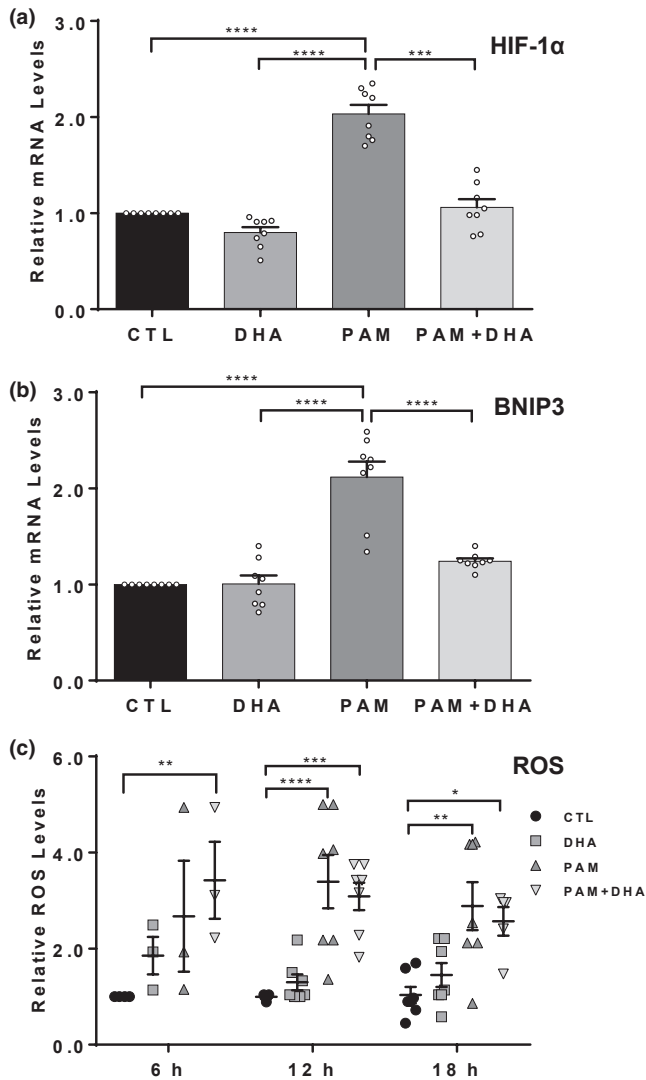


**FIGURE 6** Docosahexaenoic acid 22:6 n-3 (DHA) diminishes palmitic acid-induced lipotoxicity (PAM-LTx)-stimulated HIF-1 $\alpha$  and BNIP3 but not PAM-LTx-stimulated ROS accumulation. NGFDPC12 cells were treated with BSA control medium (CTL), DHA (50  $\mu$ M), PAM, and PAM + DHA. HIF-1 $\alpha$  (a) and BNIP3 (b) mRNA levels after 24 hr treatment were determined by real-time RT-PCR. The results are expressed as fold-change relative to control and shown as Mean  $\pm$  SEM,  $n = 8$  of independent cell culture preparations. (c) ROS levels at 6, 12, and 18 hr after treatment was determined by 2'7' dichlorodihydrofluorescein diacetate flow cytometry. The results are expressed as fold-change relative to control at 6 hr and shown as Mean  $\pm$  SEM,  $n = 3$  (6 hr) and  $n = 7$  (12 hr, 18 hr) of independent cell culture preparations. Statistical analysis was done by one-way ANOVA for figures (a) and (b) and two-way ANOVA for figure (c) followed by Bonferroni multiple comparison test. Significance symbols: \* $p < .05$ ; \*\* $p < .01$ ; \*\*\* $p < .001$ ; \*\*\*\* $p < .0001$

however, the PAM-LTx-simulated gene up-regulation of HIF-1 $\alpha$  and BNIP3 was restored to control levels in the presence of DHA (Figure 6a,b). Previous reports from our laboratory showed that intracellular ROS levels in NGFDPC12 cells are increased during PAM-LTx (Liu et al., 2015). To examine the possibility that high intracellular ROS levels are conducive to the induction of HIF-1 $\alpha$

expression in NGFDPC12 cells, we measured ROS accumulation in the cells for up to 18 hr after the indicated treatments. Figure 6c shows that PAM-LTx increased ROS levels by 3.4- and 2.9-fold at 12 and 18 hr, respectively. Interestingly, co-treatment with PAM + DHA showed an accumulation of ROS similar to PAM treatment alone (3.4-, 3.1-, and 4.2-fold at 6, 12, and 18 hr, respectively) indicating that inhibition of ROS production was not required for DHA-induced neuroprotective effects during PAM-LTx.

### 3.7 | DHA protects NGFDPC12 cells against PAM-LTx by inhibiting apoptosis and necroptosis and enhancing autophagy

As discussed earlier, the necroptosis inhibitor Nec-1 and the autophagy promoter Rapa diminished the detrimental effects of PAM-LTx in NGFDPC12 cells (Figure 3e). Thus, we hypothesized that the neuroprotective effects of DHA in the presence of PAM may involve inducing autophagy as a protective mechanism. For these experiments, we evaluated by immunoblotting the phosphorylation levels of Beclin-1, a master protein that when activated by phosphorylation inhibits apoptosis and promotes autophagy (Green & Levine, 2014). As predicted, Figure 7a shows an increase in beclin-1 phosphorylation in cells treated with Rapa and DHA. While total beclin-1 was not significantly altered upon PAM-LTx treatment, phosphobeclin-1 was greatly reduced at 48 hr in PAM-treated cells but was restored during co-treatment with DHA + PAM (Figure 7a). Next, we analyzed the conversion of light chain protein 3 (LC3-I) to phosphatidyl ethanolamine (PE)-conjugated LC3 (LC3-II), a well-established biomarker for autophagy. Immunoblotting results show a significant increase in LC3-II levels in DHA-treated but not in PAM-treated cells (Figure 7b). The lack of visible induction of LC3-II levels by rapamycin alone could be attributed to increased autophagic turnover that prevents the accumulation of LC3-II (Marino, Niso-Santano, Baehrecke, & Kroemer, 2014). However, when DHA or rapamycin were added to PAM-LTx-treated cells, the levels of LC3-II were increased. These results confirmed that DHA is able to induce autophagy in untreated or PAM-treated cells. To further analyze this autophagic process, the transcript levels of autophagy-related genes Atg7 (Figure 7c) and Atg12 (Figure 7d) were determined. Of significance, both Atg12 and Atg7 mRNA levels were reduced in PAM-treated cells, but were restored to control levels (Figure 7c) or higher than control (Figure 7d) during co-treatment with PAM and DHA.

To further assess the effects of DHA on necroptosis and autophagy we added ZVAD and chloroquine (an autophagy inhibitor) to NGFDPC12 cells exposed to either DHA or to PAM + DHA. Figure 8a shows that cell viability in the presence of DHA + ZVAD was similar to control conditions indicating that DHA inhibited ZVAD-induced necroptosis (see Figure 3a for comparison). Notably, the protective effect of DHA against PAM-LTx was diminished in the presence of chloroquine (Figure 8b), consistent with a key role for autophagy in DHA-induced protection against PAM-LTx (Figure 8b,c). We observed that NGFDPC12 cells co-treated with ZVAD and PAM exhibit

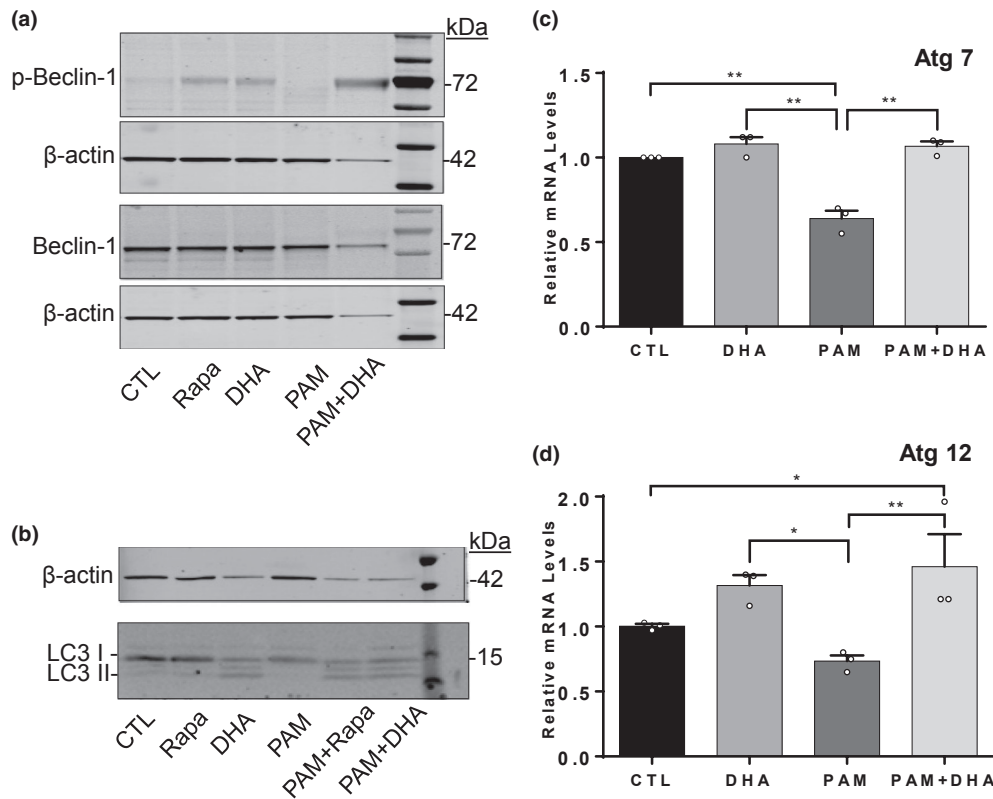


**FIGURE 7** Docosahexaenoic acid 22:6 n-3 (DHA) stimulates autophagy pathway in NGFDPC12 cells. NGFDPC12 cells were treated with BSA control medium (CTL), Rapa (100 nM), DHA (50  $\mu$ M), palmitic acid (PAM), and PAM together with Rapa or DHA for 24 hr and cellular protein was extracted. Immunoblotting analysis of (a) phosphorylated and total Beclin I and (b) LC3 were performed. Experiments were repeated at least three times and representative blots are shown. NGFDPC12 cells were treated with CTL, DHA, PAM, and PAM + DHA for 24 hr. Total cellular RNA was extracted and mRNA levels of Atg 7 (c) and Atg 12 (d) were determined by real-time RT-PCR. Results are expressed as fold-change relative to CTL and shown as mean  $\pm$  SEM,  $n = 3$  of independent cell culture preparations. Statistical analysis was done by one-way ANOVA followed by multiple comparison test. Significance symbols: \* $p < .05$ ; \*\* $p < .01$

smaller cell size, accelerated cell detachment, and fewer and shorter neurites compared to cultures treated with PAM alone (Figure 8c), consistent with the previous results (Figure 3a).

## 4 | DISCUSSION

This study reports new insights into mechanisms by which lipotoxicity induces cell death in differentiated PC12 cells, and demonstrates for the first time that the protecting effects of the n-3 PUFA DHA include inhibiting apoptosis and necroptosis, and activating autophagy. The DHA protective effect is consistent with the beneficial role of other PUFAs (e.g., EPA, ARA, and DPA), and further research to determine downstream mechanisms pertinent for each member of the family is needed.

Long chain fatty acids exhibit very low aqueous solubility but albumin which has six high-affinity-binding sites for fatty acids (Spector, John, & Fletcher, 1969) is an effective transporter in maintaining effective FA concentrations in the extracellular space (Fujiwara & Amisaki, 2013) and plays an important role in keeping a constant supply of FAs to tissues and cells (van der Vusse, 2009). Despite the high affinity of BSA for FAs, FAs can rapidly desorb from

these binding sites to be absorbed by cell membranes at the velocity of 2 to 3 milliseconds (Hamilton, 1989). For example, adding BSA to the media the cellular uptake of PAM into hepatocytes increased 14-fold compared to in the absence of BSA (Fleischer, Shurmantine, Luxon, & Forker, 1986), supporting the importance of availability of BSA-bound fatty acids for this transport process (Elmadhoun, Wang, Templeton, & Burczynski, 1998). Fatty acids are transported into the cell directly by passive diffusion involving absorption, flip-flop, and desorption. This process is assisted by fatty acid binding proteins, peroxisomes proliferator-activated receptors and cluster of differentiation 36 (CD36/SR-B2) (Glatz & Luiken, 2017). Translocation (flip-flop) seems to be the rate limiting step but with the help of CD36/SR-B2 there is increased esterification and TAG synthesis (Xu, Jay, Brunaldi, Huang, & Hamilton, 2013) specially for long chain PUFAs like DHA (Pepino, Kuda, Samovski, & Abumrad, 2014) being CD36/SR-B2 characterized in PC12 cells (Huang et al., 2019).

This study uses a well-established model for lipotoxicity to expose NGFDPC12 cells to elevated level of PAM complexed to fatty acid-free BSA (300  $\mu$ M PAM:150  $\mu$ M BSA, 2:1 ratio) which contrasts to the normal total fatty acids to serum albumin ratio of 0.75 reported in human (Richieri & Kleinfeld, 1995). This experimental approach has been shown to be an effective way to provide a robust

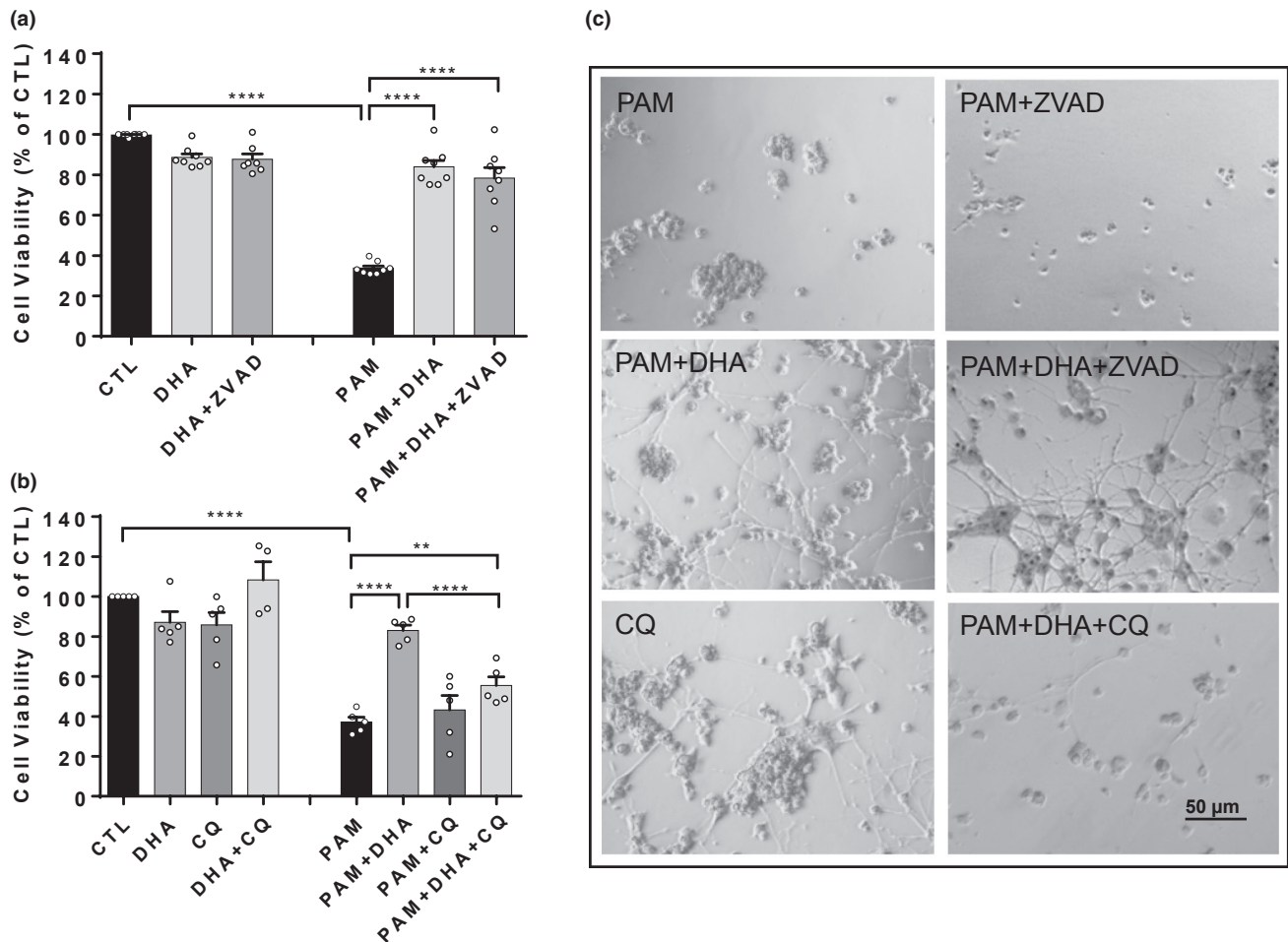


**FIGURE 8** Protective effect of docosahexaenoic acid 22:6 n-3 (DHA) in the presence of ZVAD and chloroquine in NGFDPC12 cells. NGFDPC12 cells were treated with BSA control medium (CTL), DHA, palmitic acid (PAM), and PAM + DHA in the presence or absence of ZVAD at 40  $\mu$ M (a) and chloroquine (CQ, autophagy inhibitor, 20  $\mu$ M) (b) for 48 hr. Crystal violet assay was performed to determine cell viability. Results are expressed as percent of control and shown as Mean  $\pm$  SEM,  $n = 7-8$  (a) and  $n = 4-5$  (b) of independent cell culture preparations. Statistical analysis was done by one-way ANOVA followed by multiple comparison test. Significance symbols: \*\* $p < .01$ ; \*\*\*\* $p < .0001$ . (c) Representative microscopic images show the morphology of NGFDPC12 cells 48 hr after treatments

pool of readily available PAM, BSA-bound, and -unbound combined, for intracellular accumulation which triggers lipotoxicity (Almaguel et al., 2009; Busch et al., 2005; Cnop, Hannaert, Hoorens, Eizirik, & Pipeleers, 2001; Ge et al., 2018; Hsiao, Lin, Liao, Chen, & Lin, 2014; Park, Kim, Park, & Lee, 2011; Ricchi et al., 2009; Ulloth et al., 2003). For instance, hepatocytes exposed to approximately 2:1 and 4:1 ratio of PAM:BSA showed a significant increase in cellular PAM concentration, total lipid, and triacylglycerol accumulation and caspases 3/7 activation (Ricchi et al., 2009). Similarly, PUFA:BSA at 2:1 ratio increased triacylglycerol accumulation in NGFDPC12 cells (Marszalek, Kitidis, Dararutana, & Lodish, 2004). The ability of PAM to induce lipotoxicity in NGFDPC12 cells requires it to be metabolized once transported across the cell membrane to palmitoyl-CoA, an important step necessary for the formation of phospholipids and triacylglycerols and  $\beta$ -oxidation. Indeed, while treating NGFDPC12 cells with PAM result in significant lipotoxicity and cell death, treating these cells with the non-metabolizable methyl

palmitic acid does not result in cellular ROS accumulation and cell death (Liu et al., 2015).

Once inside the cells LCSFAs bind fatty acid binding proteins and can be directed to the mitochondria for oxidation and/or to endoplasmic reticulum (ER) for complex lipid synthesis. In excess, LCSFAs may provide modification in phospholipid composition and compromise normal functions (Borradaile et al., 2006; Schenkel & Bakovic, 2014). The toxicity caused by LCSFAs may be mediated through multiple signaling cascades, such as ceramide (Sergi, Morris, & Kahn, 2018), Toll-like receptor 4/ NF $\kappa$ B pathway (Nicholas et al., 2017; Wang et al., 2012), G-protein-coupled receptor 40 (Hernandez-Caceres et al., 2019) and PI3K/AKT/mTOR (Descorbeth et al., 2018). The downstream responses include ER stress, mitochondrial and lysosomal dysfunction, and inflammation, which lead to loss of cell viability. The effects of fatty acids are affected by the degree of saturation as shown in hypothalamic cells where PAM is lipotoxic, whereas palmitoleic acid is not (Diaz et al., 2015). In human



endothelial cells palmitoleic acid, but not PAM has a strong anti-inflammatory effect (de Souza et al., 2018).

Previously, we established that treatment of NGFDPC12 cells undergoing PAM-LTx with ZVAD leads to the activation of caspase-independent cell death (Ulloth et al., 2003). This study shows for the first time that the necroptosis inhibitor Nec-1 attenuates cell death induced by ZVAD in the presence of PAM, suggesting that necroptosis is a critical cell death modality to consider in the treatment of lipotoxicity. Interestingly, we observed in this study that Nec-1 increased survival in NGFDPC12 cultures treated with ZVAD alone. ZVAD treatment decreased cell survival by 20% and treatment with Nec-1 was able to provide full recovery. We do not rule out that NGFDPC12 cells culture may be a sensitive culture model to study mechanism of necroptosis. Necroptosis is a pro-inflammatory, programmed form of cell death associated with loss of plasma membrane integrity, mitochondrial dysfunction, organelle swelling, and increase in reactive oxygen species (ROS) (Galluzzi et al., 2014; Lin et al., 2004; Shindo, Kakehashi, Okumura, Kumagai, & Nakano, 2013; Vanlangenakker et al., 2011). It can be activated by ligands of death receptors under conditions where caspase 8 activity is reduced like those observed when cells are treated with ZVAD (Galluzzi et al., 2014; Khan et al., 2014; Zhou & Yuan, 2014). Our findings that PAM overload stimulates both FAS receptor and ligand (Ulloth et al., 2003), and significantly up-regulates the accumulation of ROS ((Almaguel et al., 2010) and this study) may explain the necroptotic death activation shown in NGFDPC12 cells following an attempt to rescue them from apoptosis using ZVAD.

Our results confirmed that PAM-LTx induces apoptosis as the primary modality of cell death. However, co-treatment with Nec-1 and PAM demonstrated a modest but significant protection even in the absence of ZVAD. Nec-1 is a very specific small molecule inhibitor of RIP1 (Degterev et al., 2008; He et al., 2009). RIP1, through its death domain, complexes with FADD (Fas-associated protein with death domain) and TRADD (tumor necrosis factor receptor-associated death domain) (Stanger, Leder, Lee, Kim, & Seed, 1995) and binds caspase 8 to form the ripoptosome which is necessary for the extrinsic apoptotic pathway (Khan et al., 2014). Inhibition of RIP1 kinase activity by Nec-1 suppresses apoptosis by preventing the formation of RIP1/FADD/caspase 8 cell death complex also known as Complex IIa (Abhari et al., 2013; Feoktistova et al., 2011). Along these lines, rats treated with Nec-1 before spinal cord injury showed a smaller lesion size, inhibition of cytokine release and decreased ROS production (Wang et al., 2014). These outcomes were accompanied by a reduction in caspase 3 and Bax and an activation of the anti-apoptotic and autophagy-modulator protein Bcl-2 (Wang et al., 2014). Since both extrinsic (Fas-mediated) and intrinsic (mitochondrial-mediated) apoptosis pathways are evident during PAM-LTx in NGFDPC12 cells (Almaguel et al., 2009; Ulloth et al., 2003), we cannot rule out that Nec-1, in the absence of ZVAD, increases cell viability under PAM-LTx by attenuating Fas-mediated apoptosis. On the other hand, ZVAD does not rescue NGFDPC12 cells exposed to PAM because of its inhibition of caspase 8. Caspase 8 has been shown to cleave the necroptosis-associated proteins RIP1, RIP3, and

MLKL (Khan et al., 2014), and Nec-1 inhibits RIP1, decreasing MLKL phosphorylation in the necroptosome.

We found that co-treatment with Nec-1 and rapamycin successfully rescued NGFDPC12 cells undergoing PAM-LTx, suggesting that activation of autophagy is critical in neuroprotection against lipotoxicity. Rapamycin is a macrolide that inhibits mTOR, a serine/threonine protein kinase that regulates autophagy, cell growth, and cell proliferation (Mukherjee & Mukherjee, 2009). When mTOR is inhibited, the ULK1 complex (UNC-51-like kinase 1 + ATG17 + ATG13 + ATG101) is free to stimulate the autophagic cascade (Marino et al., 2014). Autophagy is particularly important in neurons because as non-dividing cells are more sensitive to accumulation of toxic molecules, and cells in the brain need a constant supply of energy even under stressful conditions like ischemia, starvation, or infection (Hara et al., 2006). Inhibition of autophagy causes neurodegeneration in mature neurons, indicating that autophagy may regulate neuronal homeostasis (Komatsu et al., 2006).

There are multiple stress signals that can also exhibit the involvement of both autophagy and apoptosis (Tan et al., 2012; Tu et al., 2014). For example, the Bcl-2-binding factor Beclin-1 (ATG6) is the central protein regulating the autophagy process. Beclin-1 associates with VPS34 (vacuolar protein sorting 34) and initiates the isolation of double membranes to start autophagy. This Beclin-1/VPS34 complex is inhibited when bound by Bcl-2 family members (Bcl-2, Bcl-X<sub>L</sub>) establishing a check-and-balance system that ensures that autophagy is activated only when cells are under stress conditions. This complex prevents the process to turn into (hyper) autophagy (Green & Levine, 2014; Luo & Rubinsztein, 2010; Maiuri et al., 2007). In a T-cell model lacking caspase 8 and FADD, cells developed a hyperautophagic morphology and cells subsequently died by necroptosis that can be prevented with necroptosis inhibitors and deletion of RIP3 (Lu et al., 2011). In our studies, rapamycin by itself did not rescue NGFDPC12 cells from PAM-LTx probably because of its inability to prevent the hyper-autophagy status that could activate necroptosis. This finding would explain that co-treatment with Nec-1 and rapamycin was the most effective treatment to rescue cells from PAM-LTx. It is not speculative to propose that apoptosis-activated caspases may digest essential autophagic proteins and disable the autophagy pathway if the cells are exposed to a strong stressor that overrides the cellular capability to activate autophagy (Long & Ryan, 2012).

We also report in this study that n-3 PUFAs (DHA, EPA, and n-3 DPA) and n-6 PUFA (ARA), but not n-6 DPA, protect NGFDPC12 cells cultures from PAM-LTx. Because of the curved structure provided by PUFAs, enrichment of PUFA-containing phospholipids increases membrane fluidity and facilitates lateral diffusion of membrane proteins. This biophysical effect decreases membrane thickness and increases permeability to ions and small molecules, contributing an essential role in various neurochemical processes and protein transport and activities of nerve cell membranes (Bazan, Marcheselli, & Cole-Edwards, 2005; Hishikawa, Valentine, Iizuka-Hishikawa, Shindou, & Shimizu, 2017; Nishio et al., 2004; Spector & Yorek, 1985; Vasquez, Krieg, Lockhead, & Goodman, 2014).

Biomembrane analysis have shown that EPA-containing phosphatylcholines exhibit the highest disorder among the three n-3 PUFAs (Leng et al., 2018) and DHA-containing phosphatylcholines modify the molecular organization of sphingomyelin/cholesterol-enriched lipid rafts, but not the oleate counterpart (Wassall et al., 2018). The metabolism of n-3 and n-6 PUFAs share the same series of enzymes, competition between n-3 and n-6 PUFAs occurs in the process and deficiencies in the supply of n-3 fatty acids results in replacement of DHA by n-6 DPA in brain membrane (Moriguchi, Greiner, & Salem, 2000). Interestingly, this slight difference in the chemical structure of n-3 and n-6 fatty acids results in significant alterations in membrane structure and therefore in its biophysical properties (Eldho, Feller, Tristram-Nagle, Polozov, & Gawrisch, 2003).

A previous report shows that DHA, EPA, and ARA, but not oleate, potentiate neurite expansion in NGFDPC12 cells, which seemed to be mediated through epidermal fatty acid binding protein (FABP5) (Liu, Almaguel, Bu, De Leon, & De Leon, 2008). FABP5 expression was shown to be stimulated by the oxidative stress that followed PAM exposure, and increased levels of this protein were neuroprotective (Liu et al., 2008). The peroxisome proliferator-activated receptor gamma (PPAR $\gamma$ ) agonist rescues NGFDPC12 cells from PAM-LTx, which coincides with the up-regulation of FABP5 (Liu et al., 2015). These findings are consistent with reports regarding the role of PPAR $\gamma$  in neuroprotection because of its ability to decrease oxidative stress and inflammatory response (Bordet et al., 2006). The n-3 and n-6 PUFAs and their metabolites are natural ligands for PPAR $\gamma$  (Marion-Letellier, Savoye, & Ghosh, 2016) and activating PPAR $\gamma$  may mediate the neuroprotective effects of DHA and ARA (Sun et al., 2015; Wang, Liang, Li, Yu, & Yin, 2006; Zhao et al., 2011). Membrane phospholipids serve as a reservoir of n-3 and n-6 fatty acids that are released by phospholipase A2 activation. DHA, EPA, and ARA are precursors to diverse bioactive lipid mediators like, resolvins, neuroprotection D-1, maresins, E-series resolvins, and endocannabinoids. Therefore, the levels of phospholipid-bound PUFAs determine the levels of their subsequent metabolites and biological functions (Dyall, 2017; Freitas et al., 2018).

A novel finding from this study is that the protective effects of DHA against PAM-LTx are mediated by impacting multiple cellular pathways, that is, inhibition of apoptosis and necroptosis, and stimulation of autophagy. These findings are in agreement with previous results showing that DHA inhibited mitochondrial membrane depolarization and lysosomal membrane permeabilization (Almaguel et al., 2010). While we found that PAM-LTx induces the expression of HIF-1 $\alpha$  and BNIP-3, treatment with DHA reduced the transcript levels for both genes. HIF-1 $\alpha$  functions as a cellular stress sensor that induces the expression of cell survival genes and/or cell death genes (Guo, 2017). While HIF-1 $\alpha$  can promote autophagy directly through the HIF-1 $\alpha$ /BNIP3/Beclin-1 complex, which involves the mTOR signaling (Xia et al., 2015), it can also induce apoptosis (da Rosa et al., 2015). In our cellular model of lipotoxicity, PAM decreased Beclin-1 phosphorylation, suggesting that it decreases autophagy and activates apoptosis through the induction of HIF1 $\alpha$  and BNIP3 expression. In contrast, treatment

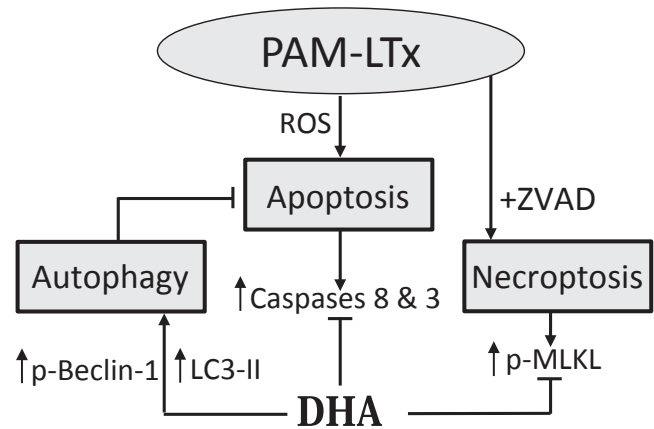


**FIGURE 9** The neuroprotective function of docosahexaenoic acid 22:6 n-3 (DHA) during PAM-induced lipotoxicity includes inhibition of apoptosis and necroptosis and stimulation of autophagy

with DHA in the presence of PAM inhibited the expression of these two genes, suggesting that by inducing autophagy DHA antagonizes cell death processes associated with increased HIF1 $\alpha$  and BNIP3 expression and activity.

In our experimental model, DHA elicited a small and transient increase in ROS accumulation and did not inhibit the ROS generation observed during PAM-LTx conditions. Interestingly, studies performed in human retinal pigment epithelial cells showed that DHA triggers a transient increase in ROS, and an increase in the levels of nuclear translocation of NFE2L2, a transcription factor that regulates cellular redox status (Johansson et al., 2015). Subsequently, DHA was shown to increase the levels of SQSTM1, which selectively targets misfolded, ubiquitinated proteins for lysosomal degradation by binding both to ubiquitinated cargos and to LC3 (Atg8) on the growing phagophore membrane (Johansson et al., 2015). LC3-II, which is phosphatidyl ethanolamine (PE)-conjugated, is responsible for docking the autophagosome with the lysosome vesicles. Thus, DHA-containing PE can facilitate this process as opposed to saturated fatty acid-containing PE (Garcia, Ward, Ma, Salem, & Kim, 1998; Kim, Bigelow, & Kevala, 2004).

In summary, the findings reported in this study provide evidence suggesting that the protective role of DHA during lipotoxicity includes the inhibition of apoptosis and necroptosis and stimulation of autophagy (Figure 9). n-3 PUFAs have been proposed to play various neuroprotective roles during traumatic injuries in the nervous system and neurodegenerative diseases. We propose that the neuroprotective effects of DHA and other PUFAs may involve the activation and regulation of these critical cell death and survival pathways.

#### ACKNOWLEDGMENTS

Research reported in this publication was supported by the National Institute of General Medical Sciences and National Institutes on Minority Health and Health Disparities of the National Institutes of Health under award Numbers R25GM060507 and P20MD006988,



respectively. The content is solely the responsibility of the authors and does not necessarily represent the official views of the National Institutes of Health.

All experiments were conducted in compliance with the ARRIVE guidelines.

## CONFLICT OF INTEREST

The authors declare that there is no conflict of interest.

## ORCID

Marino De Leon  <https://orcid.org/0000-0002-2742-2786>

## REFERENCES

- Abhari, B. A., Cristofanon, S., Kappler, R., von Schweinitz, D., Humphreys, R., & Fulda, S. (2013). RIP1 is required for IAP inhibitor-mediated sensitization for TRAIL-induced apoptosis via a RIP1/FADD/caspase-8 cell death complex. *Oncogene*, *32*, 3263–3273. <https://doi.org/10.1038/onc.2012.337>
- Almague, F. G., Liu, J. W., Pacheco, F. J., Casiano, C. A., & De Leon, M. (2009). Activation and reversal of lipotoxicity in PC12 and rat cortical cells following exposure to palmitic acid. *Journal of Neuroscience Research*, *87*, 1207–1218. <https://doi.org/10.1002/jnr.21918>
- Almague, F. G., Liu, J. W., Pacheco, F. J., De Leon, D., Casiano, C. A., & De Leon, M. (2010). Lipotoxicity-mediated cell dysfunction and death involve lysosomal membrane permeabilization and cathepsin L activity. *Brain Research*, *1318*, 133–143. <https://doi.org/10.1016/j.brainres.2009.12.038>
- Bazan, N. G., Marcheselli, V. L., & Cole-Edwards, K. (2005). Brain response to injury and neurodegeneration: Endogenous neuroprotective signaling. *Annals of the New York Academy of Sciences*, *1053*, 137–147. <https://doi.org/10.1196/annals.1344.011>
- Berghe, T. V., Vanlangenakker, N., Parthoens, E., Deckers, W., Devos, M., Festjens, N., ... Vandenabeele, P. (2010). Necroptosis, necrosis and secondary necrosis converge on similar cellular disintegration features. *Cell Death and Differentiation*, *17*, 922–930. <https://doi.org/10.1038/cdd.2009.184>
- Bordet, R., Ouk, T., Petrault, O., Gelé, P., Gautier, S., Laprais, M., ... Bastide, M. (2006). PPAR: A new pharmacological target for neuroprotection in stroke and neurodegenerative diseases. *Biochemical Society Transactions*, *34*, 1341–1346. <https://doi.org/10.1042/BST0341341>
- Borradaile, N. M., Han, X., Harp, J. D., Gale, S. E., Ory, D. S., & Schaffer, J. E. (2006). Disruption of endoplasmic reticulum structure and integrity in lipotoxic cell death. *Journal of Lipid Research*, *47*, 2726–2737. <https://doi.org/10.1194/jlr.M600299-JLR200>
- Bray, K., Mathew, R., Lau, A., Kamphorst, J. J., Fan, J., Chen, J., ... White, E. (2012). Autophagy suppresses RIP kinase-dependent necrosis enabling survival to mTOR inhibition. *PLoS ONE*, *7*, e41831. <https://doi.org/10.1371/journal.pone.0041831>
- Busch, A. K., Gurisik, E., Cordery, D. V., Sudlow, M., Denyer, G. S., Laybutt, D. R., ... Biden, T. J. (2005). Increased fatty acid desaturation and enhanced expression of stearoyl coenzyme A desaturase protects pancreatic beta-cells from lipoapoptosis. *Diabetes*, *54*, 2917–2924.
- Casiano, C. A., Martin, S. J., Green, D. R., & Tan, E. M. (1996). Selective cleavage of nuclear autoantigens during CD95 (Fas/APO-1)-mediated T cell apoptosis. *Journal of Experimental Medicine*, *184*, 765–770. <https://doi.org/10.1084/jem.184.2.765>
- Casiano, C. A., Ochs, R. L., & Tan, E. M. (1998). Distinct cleavage products of nuclear proteins in apoptosis and necrosis revealed by autoantibody probes. *Cell Death and Differentiation*, *5*, 183–190. <https://doi.org/10.1038/sj.cdd.4400336>
- Cnop, M., Hannaert, J. C., Hoorens, A., Eizirik, D. L., & Pipeleers, D. G. (2001). Inverse relationship between cytotoxicity of free fatty acids in pancreatic islet cells and cellular triglyceride accumulation. *Diabetes*, *50*, 1771–1777. <https://doi.org/10.2337/diabetes.50.8.1771>
- da Rosa, D. P., Forgiarini, L. F., e Silva, M. B., Fiori, C. Z., Andrade, C. F., Martinez, D., & Marroni, N. P. (2015). Antioxidants inhibit the inflammatory and apoptotic processes in an intermittent hypoxia model of sleep apnea. *Inflammation Research*, *64*, 21–29. <https://doi.org/10.1007/s00011-014-0778-5>
- Damme, M., Suntuio, T., Saftig, P., & Eskelinen, E. L. (2014). Autophagy in neuronal cells: General principles and physiological and pathological functions. *Acta Neuropathologica*. <https://doi.org/10.1007/s00401-014-1361-4>
- de Souza, C. O., Valenzuela, C. A., Baker, E. J., Miles, E. A., Rosa Neto, J. C., & Calder, P. C. (2018). Palmitoleic acid has stronger anti-inflammatory potential in human endothelial cells compared to oleic and palmitic acids. *Molecular Nutrition and Food Research*, *62*, e1800322. <https://doi.org/10.1002/mnfr.201800322>
- Degenhardt, K., Mathew, R., Beaudoin, B., Bray, K., Anderson, D., Chen, G., ... White, E. (2006). Autophagy promotes tumor cell survival and restricts necrosis, inflammation, and tumorigenesis. *Cancer Cell*, *10*, 51–64. <https://doi.org/10.1016/j.ccr.2006.06.001>
- Degtarev, A., Hitomi, J., Germscheid, M., Ch'en, I. L., Korkina, O., Teng, X., ... Yuan, J. (2008). Identification of RIP1 kinase as a specific cellular target of necrostatins. *Nature Chemical Biology*, *4*, 313–321. <https://doi.org/10.1038/nchembio.83>
- Descorbeth, M., Figueroa, K., Serrano-Illan, M., & De Leon, M. (2018). Protective effect of docosahexaenoic acid on lipotoxicity-mediated cell death in Schwann cells: Implication of PI3K/AKT and mTORC2 pathways. *Brain and Behavior*, *8*, e01123. <https://doi.org/10.1002/brb3.1123>
- Dhillon, H. S., Dose, J. M., Scheff, S. W., & Prasad, M. R. (1997). Time course of changes in lactate and free fatty acids after experimental brain injury and relationship to morphological damage. *Experimental Neurology*, *146*, 240–249. <https://doi.org/10.1006/exnr.1997.6524>
- Diaz, B., Fuentes-Mera, L., Tovar, A., Montiel, T., Massieu, L., Martinez-Rodriguez, H. G., & Camacho, A. (2015). Saturated lipids decrease mitofusin 2 leading to endoplasmic reticulum stress activation and insulin resistance in hypothalamic cells. *Brain Research*, *1627*, 80–89. <https://doi.org/10.1016/j.brainres.2015.09.014>
- Djavaheri-Mergny, M., Maiuri, M. C., & Kroemer, G. (2010). Cross talk between apoptosis and autophagy by caspase-mediated cleavage of Beclin 1. *Oncogene*, *29*, 1717–1719. <https://doi.org/10.1038/onc.2009.519>
- Dyall, S. C. (2017). Interplay between n-3 and n-6 long-chain polyunsaturated fatty acids and the endocannabinoid system in brain protection and repair. *Lipids*, *52*, 885–900. <https://doi.org/10.1007/s11745-017-4292-8>
- Eguchi, Y., Shimizu, S., & Tsujimoto, Y. (1997). Intracellular ATP levels determine cell death fate by apoptosis or necrosis. *Cancer Research*, *57*, 1835–1840.
- Eldho, N. V., Feller, S. E., Tristram-Nagle, S., Polozov, I. V., & Gawrisch, K. (2003). Polyunsaturated docosahexaenoic vs docosapentaenoic acid-differences in lipid matrix properties from the loss of one double bond. *Journal of the American Chemical Society*, *125*, 6409–6421. <https://doi.org/10.1021/ja029029o>
- Elmadhoun, B. M., Wang, G. Q., Templeton, J. F., & Burczynski, F. J. (1998). Binding of [3H]palmitate to BSA. *American Journal of Physiology*, *275*, G638–644.
- Feltham, R., Vince, J. E., & Lawlor, K. E. (2017). Caspase-8: Not so silently deadly. *Clinical and Translational Immunology*, *6*, e124. <https://doi.org/10.1038/cti.2016.83>
- Foektistova, M., Geserick, P., Kellert, B., Dimitrova, D. P., Langlais, C., Hupe, M., ... Leverkus, M. (2011). cIAPs block Ripoptosome formation, a RIP1/caspase-8 containing intracellular cell death complex differentially regulated by cFLIP isoforms. *Molecular Cell*, *43*, 449–463. <https://doi.org/10.1016/j.molcel.2011.06.011>

- Figueroa, J. D., Cordero, K., Baldeosingh, K., Torrado, A. I., Walker, R. L., Miranda, J. D., & Leon, M. D. (2012). Docosahexaenoic acid pretreatment confers protection and functional improvements after acute spinal cord injury in adult rats. *Journal of Neurotrauma*, *29*, 551–566. <https://doi.org/10.1089/neu.2011.2141>
- Figueroa, J. D., Cordero, K., Llan, M. S., & De Leon, M. (2013). Dietary omega-3 polyunsaturated fatty acids improve the neurolipidome and restore the DHA status while promoting functional recovery after experimental spinal cord injury. *Journal of Neurotrauma*, *30*, 853–868. <https://doi.org/10.1089/neu.2012.2718>
- Figueroa, J. D., Cordero, K., Serrano-Illan, M., Almeida, A., Baldeosingh, K., Almague, F. G., & De Leon, M. (2013). Metabolomics uncovers dietary omega-3 fatty acid-derived metabolites implicated in anti-nociceptive responses after experimental spinal cord injury. *Neuroscience*, *255*, 1–18. <https://doi.org/10.1016/j.neuroscience.2013.09.012>
- Fleischer, A. B., Shurmantine, W. O., Luxon, B. A., & Foraker, E. L. (1986). Palmitate uptake by hepatocyte monolayers. Effect of albumin binding. *Journal of Clinical Investigation*, *77*, 964–970. <https://doi.org/10.1172/JCI112397>
- Freitas, H. R., Isaac, A. R., Malcher-Lopes, R., Diaz, B. L., Trevenzoli, I. H., & De Melo Reis, R. A. (2018). Polyunsaturated fatty acids and endocannabinoids in health and disease. *Nutritional Neuroscience*, *21*, 695–714. <https://doi.org/10.1080/1028415X.2017.1347373>
- Fujiwara, S., & Amisaki, T. (2013). Fatty acid binding to serum albumin: Molecular simulation approaches. *Biochimica et Biophysica Acta (BBA) - General Subjects*, *1830*, 5427–5434. <https://doi.org/10.1016/j.bbagen.2013.03.032>
- Galluzzi, L., Kepp, O., Krautwald, S., Kroemer, G., & Linkermann, A. (2014). Molecular mechanisms of regulated necrosis. *Seminars in Cell and Developmental Biology*, *35*, 24–32. <https://doi.org/10.1016/j.semdb.2014.02.006>
- Garcia, M. C., Ward, G., Ma, Y. C., Salem, N. Jr, & Kim, H. Y. (1998). Effect of docosahexaenoic acid on the synthesis of phosphatidylserine in rat brain in microsomes and C6 glioma cells. *Journal of Neurochemistry*, *70*, 24–30.
- Ge, X., Pan, P., Jing, J., Hu, X., Chen, L. I., Qiu, X., ... Yao, B. (2018). Rosiglitazone ameliorates palmitic acid-induced cytotoxicity in TM4 Sertoli cells. *Reproductive Biology and Endocrinology*, *16*, 98. <https://doi.org/10.1186/s12958-018-0416-0>
- Glatz, J. F., & Luiken, J. J. (2017). From fat to FAT (CD36/SR-B2): Understanding the regulation of cellular fatty acid uptake. *Biochimie*, *136*, 21–26. <https://doi.org/10.1016/j.biochi.2016.12.007>
- Green, D. R., & Levine, B. (2014). To be or not to be? How selective autophagy and cell death govern cell fate. *Cell*, *157*, 65–75. <https://doi.org/10.1016/j.cell.2014.02.049>
- Guo, Y. (2017). Role of HIF-1 $\alpha$  in regulating autophagic cell survival during cerebral ischemia reperfusion in rats. *Oncotarget*, *8*, 98482–98494. <https://doi.org/10.18632/oncotarget.21445>
- Hamilton, J. A. (1989). Medium-chain fatty acid binding to albumin and transfer to phospholipid bilayers. *Proceedings of the National Academy of Sciences of the United States of America*, *86*, 2663–2667. <https://doi.org/10.1073/pnas.86.8.2663>
- Han, J., & Kaufman, R. J. (2016). The role of ER stress in lipid metabolism and lipotoxicity. *Journal of Lipid Research*, *57*, 1329–1338. <https://doi.org/10.1194/jlr.R067595>
- Hara, T., Nakamura, K., Matsui, M., Yamamoto, A., Nakahara, Y., Suzuki-Migishima, R., ... Mizushima, N. (2006). Suppression of basal autophagy in neural cells causes neurodegenerative disease in mice. *Nature*, *441*, 885–889. <https://doi.org/10.1038/nature04724>
- He, S., Wang, L., Miao, L., Wang, T., Du, F., Zhao, L., & Wang, X. (2009). Receptor interacting protein kinase-3 determines cellular necrotic response to TNF- $\alpha$ . *Cell*, *137*, 1100–1111.
- Hernández-Cáceres, M. P., Toledo-Valenzuela, L., Díaz-Castro, F., Ávalos, Y., Burgos, P., Narro, C., ... Morselli, E. (2019). Palmitic acid reduces the autophagic flux and insulin sensitivity through the activation of the free fatty acid receptor 1 (FFAR1) in the hypothalamic neuronal cell line N43/5. *Front Endocrinol (Lausanne)*, *10*, 176. <https://doi.org/10.3389/fendo.2019.00176>
- Hishikawa, D., Valentine, W. J., Iizuka-Hishikawa, Y., Shindou, H., & Shimizu, T. (2017). Metabolism and functions of docosahexaenoic acid-containing membrane glycerophospholipids. *FEBS Letters*, *591*, 2730–2744. <https://doi.org/10.1002/1873-3468.12825>
- Holler, N., Zaru, R., Mischeau, O., Thome, M., Attinger, A., Valitutti, S., ... Tschopp, J. (2000). Fas triggers an alternative, caspase-8-independent cell death pathway using the kinase RIP as effector molecule. *Nature Immunology*, *1*, 489–495. <https://doi.org/10.1038/82732>
- Hsiao, Y. H., Lin, C. I., Liao, H., Chen, Y. H., & Lin, S. H. (2014). Palmitic acid-induced neuron cell cycle G2/M arrest and endoplasmic reticular stress through protein palmitoylation in SH-SY5Y human neuroblastoma cells. *International Journal of Molecular Sciences*, *15*, 20876–20899. <https://doi.org/10.3390/ijms151120876>
- Huang, X., Zhen, J., Dong, S., Zhang, H., Van Halm-Lutterodt, N., & Yuan, L. (2019). DHA and vitamin E antagonized the Abeta25-35-mediated neuron oxidative damage through activation of Nrf2 signaling pathways and regulation of CD36, SRB1 and FABP5 expression in PC12 cells. *Food and Function*, *10*, 1049–1061.
- Johansson, I., Monsen, V. T., Pettersen, K., Mildnerberger, J., Misund, K., Kaarniranta, K., ... Bjorkoy, G. (2015). The marine n-3 PUFA DHA evokes cytoprotection against oxidative stress and protein misfolding by inducing autophagy and NFE2L2 in human retinal pigment epithelial cells. *Autophagy*, *11*, 1636–1651. <https://doi.org/10.1080/15548627.2015.1061170>
- Khan, N., Lawlor, K. E., Murphy, J. M., & Vince, J. E. (2014). More to life than death: Molecular determinants of necroptotic and non-necroptotic RIP3 kinase signaling. *Current Opinion in Immunology*, *26*, 76–89. <https://doi.org/10.1016/j.coi.2013.10.017>
- Kim, H. Y., Bigelow, J., & Kevala, J. H. (2004). Substrate preference in phosphatidylserine biosynthesis for docosahexaenoic acid containing species. *Biochemistry*, *43*, 1030–1036. <https://doi.org/10.1021/bi035197x>
- Komatsu, M., Waguri, S., Chiba, T., Murata, S., Iwata, J.-I., Tanida, I., ... Tanaka, K. (2006). Loss of autophagy in the central nervous system causes neurodegeneration in mice. *Nature*, *441*, 880–884. <https://doi.org/10.1038/nature04723>
- Lauritzen, I., Blondeau, N., Heurteaux, C., Widmann, C., Romey, G., & Lazdunski, M. (2000). Polyunsaturated fatty acids are potent neuroprotectors. *The EMBO Journal*, *19*, 1784–1793. <https://doi.org/10.1093/emboj/19.8.1784>
- Leist, M., Single, B., Castoldi, A. F., Kühnle, S., & Nicotera, P. (1997). Intracellular adenosine triphosphate (ATP) concentration: A switch in the decision between apoptosis and necrosis. *Journal of Experimental Medicine*, *185*, 1481–1486. <https://doi.org/10.1084/jem.185.8.1481>
- Leng, X., Kinnun, J. J., Cavazos, A. T., Canner, S. W., Shaikh, S. R., Feller, S. E., & Wassall, S. R. (2018). All n-3 PUFA are not the same: MD simulations reveal differences in membrane organization for EPA, DHA and DPA. *Biochimica et Biophysica Acta (BBA) - Biomembranes*, *1860*, 1125–1134. <https://doi.org/10.1016/j.bbamem.2018.01.002>
- Leroy, C., Tricot, S., Lacour, B., & Grynberg, A. (2008). Protective effect of eicosapentaenoic acid on palmitate-induced apoptosis in neonatal cardiomyocytes. *Biochimica et Biophysica Acta (BBA) - Molecular and Cell Biology of Lipids*, *1781*, 685–693. <https://doi.org/10.1016/j.bbailip.2008.07.009>
- Lin, Y., Choksi, S., Shen, H. M., Yang, Q. F., Hur, G. M., Kim, Y. S., ... Liu, Z. G. (2004). Tumor necrosis factor-induced nonapoptotic cell death requires receptor-interacting protein-mediated cellular reactive oxygen species accumulation. *Journal of Biological Chemistry*, *279*, 10822–10828. <https://doi.org/10.1074/jbc.M313141200>
- Linkermann, A., Brasen, J. H., De Zen, F., Weinlich, R., Schwendener, R. A., Green, D. R., ... Krautwald, S. (2012). Dichotomy between RIP1- and



- RIP3-mediated necroptosis in tumor necrosis factor-alpha-induced shock. *Molecular Medicine*, 18, 577–586.
- Listenberger, L. L., & Schaffer, J. E. (2002). Mechanisms of lipopoptosis: Implications for human heart disease. *Trends in Cardiovascular Medicine*, 12, 134–138. [https://doi.org/10.1016/S1050-1738\(02\)00152-4](https://doi.org/10.1016/S1050-1738(02)00152-4)
- Liu, J. W., Almaguel, F. G., Bu, L., De Leon, D. D., & De Leon, M. (2008). Expression of E-FABP in PC12 cells increases neurite extension during differentiation: Involvement of n-3 and n-6 fatty acids. *Journal of Neurochemistry*, 106, 2015–2029. <https://doi.org/10.1111/j.1471-4159.2008.05507.x>
- Liu, J. W., Montero, M., Bu, L., & De Leon, M. (2015). Epidermal fatty acid-binding protein protects nerve growth factor-differentiated PC12 cells from lipotoxic injury. *Journal of Neurochemistry*, 132, 85–98. <https://doi.org/10.1111/jnc.12934>
- Long, J. S., & Ryan, K. M. (2012). New frontiers in promoting tumour cell death: Targeting apoptosis, necroptosis and autophagy. *Oncogene*, 31, 5045–5060. <https://doi.org/10.1038/onc.2012.7>
- Lu, J. V., Weist, B. M., van Raam, B. J., Marro, B. S., Nguyen, L. V., Srinivas, P., ... Walsh, C. M. (2011). Complementary roles of Fas-associated death domain (FADD) and receptor interacting protein kinase-3 (RIPK3) in T-cell homeostasis and antiviral immunity. *Proceedings of the National Academy of Sciences of the United States of America*, 108, 15312–15317. <https://doi.org/10.1073/pnas.1102779108>
- Luo, S., & Rubinsztein, D. C. (2010). Apoptosis blocks Beclin 1-dependent autophagosome synthesis: An effect rescued by Bcl-xL. *Cell Death and Differentiation*, 17, 268–277. <https://doi.org/10.1038/cdd.2009.121>
- Maiuri, M. C., Le Toumelin, G., Criollo, A., Rain, J.-C., Gautier, F., Juin, P., ... Kroemer, G. (2007). Functional and physical interaction between Bcl-X(L) and a BH3-like domain in Beclin-1. *The EMBO Journal*, 26, 2527–2539. <https://doi.org/10.1038/sj.emboj.7601689>
- Marino, G., Niso-Santano, M., Baehrecke, E. H., & Kroemer, G. (2014). Self-consumption: The interplay of autophagy and apoptosis. *Nature Reviews Molecular Cell Biology*, 15, 81–94. <https://doi.org/10.1038/nrm3735>
- Marion-Letellier, R., Savoye, G., & Ghosh, S. (2016). Fatty acids, eicosanoids and PPAR gamma. *European Journal of Pharmacology*, 785, 44–49. <https://doi.org/10.1016/j.ejphar.2015.11.004>
- Marszalek, J. R., Kitidis, C., Dararutana, A., & Lodish, H. F. (2004). Acyl-CoA synthetase 2 overexpression enhances fatty acid internalization and neurite outgrowth. *Journal of Biological Chemistry*, 279, 23882–23891. <https://doi.org/10.1074/jbc.M313460200>
- Meng, M.-B., Wang, H.-H., Cui, Y.-L., Wu, Z.-Q., Shi, Y.-Y., Zaorsky, N. G., ... Wang, P. (2016). Necroptosis in tumorigenesis, activation of anti-tumor immunity, and cancer therapy. *Oncotarget*, 7, 57391–57413. <https://doi.org/10.18632/oncotarget.10548>
- Moriguchi, T., Greiner, R. S., & Salem, N. Jr (2000). Behavioral deficits associated with dietary induction of decreased brain docosahexaenoic acid concentration. *Journal of Neurochemistry*, 75, 2563–2573. <https://doi.org/10.1046/j.1471-4159.2000.0752563.x>
- Mukherjee, S., & Mukherjee, U. (2009). A comprehensive review of immunosuppression used for liver transplantation. *Journal of Transplantation*, 2009, 701464. <https://doi.org/10.1155/2009/701464>
- Newton, K., Dugger, D. L., Wickliffe, K. E., Kapoor, N., de Almagro, M. C., Vucic, D., ... Dixit, V. M. (2014). Activity of protein kinase RIPK3 determines whether cells die by necroptosis or apoptosis. *Science*, 343, 1357–1360. <https://doi.org/10.1126/science.1249361>
- Nicholas, D. A., Zhang, K., Hung, C., Glasgow, S., Aruni, A. W., Unternaehrer, J., ... De Leon, M. (2017). Palmitic acid is a toll-like receptor 4 ligand that induces human dendritic cell secretion of IL-1beta. *PLoS ONE*, 12, e0176793.
- Nishio, M., Fukumoto, S., Furukawa, K., Ichimura, A., Miyazaki, H., Kusunoki, S., ... Furukawa, K. (2004). Overexpressed GM1 suppresses nerve growth factor (NGF) signals by modulating the intracellular localization of NGF receptors and membrane fluidity in PC12 cells. *Journal of Biological Chemistry*, 279, 33368–33378. <https://doi.org/10.1074/jbc.M403816200>
- Northington, F. J., Chavez-Valdez, R., Graham, E. M., Razdan, S., Gauda, E. B., & Martin, L. J. (2011). Necrostatin decreases oxidative damage, inflammation, and injury after neonatal HI. *Journal of Cerebral Blood Flow and Metabolism*, 31, 178–189. <https://doi.org/10.1038/jcbfm.2010.72>
- Oerlemans, M. I., Liu, J., Arslan, F., den Ouden, K., van Middelaar, B. J., Doevendans, P. A., & Sluijter, J. P. (2012). Inhibition of RIP1-dependent necrosis prevents adverse cardiac remodeling after myocardial ischemia-reperfusion in vivo. *Basic Research in Cardiology*, 107, 270. <https://doi.org/10.1007/s00395-012-0270-8>
- Pacheco, F. J., Almaguel, F. G., Evans, W., Rios-Colon, L., Filipov, V., Leoh, L. S., ... Casiano, C. A. (2014). Docosahexanoic acid antagonizes TNF-alpha-induced necroptosis by attenuating oxidative stress, ceramide production, lysosomal dysfunction, and autophagic features. *Inflammation Research*, 63, 859–871.
- Pacheco, F. J., Servin, J., Dang, D., Kim, J., Molinaro, C., Daniels, T., ... Casiano, C. A. (2005). Involvement of lysosomal cathepsins in the cleavage of DNA topoisomerase I during necrotic cell death. *Arthritis and Rheumatism*, 52, 2133–2145. <https://doi.org/10.1002/art.21147>
- Padilla, A., Descorbeth, M., Almeyda, A. L., Payne, K., & De Leon, M. (2011). Hyperglycemia magnifies Schwann cell dysfunction and cell death triggered by PA-induced lipotoxicity. *Brain Research*, 1370, 64–79. <https://doi.org/10.1016/j.brainres.2010.11.013>
- Park, H. R., Kim, J. Y., Park, K. Y., & Lee, J. (2011). Lipotoxicity of palmitic Acid on neural progenitor cells and hippocampal neurogenesis. *Toxicological Research*, 27, 103–110. <https://doi.org/10.5487/TR.2011.27.2.103>
- Patil, S., & Chan, C. (2005). Palmitic and stearic fatty acids induce Alzheimer-like hyperphosphorylation of tau in primary rat cortical neurons. *Neuroscience Letters*, 384, 288–293. <https://doi.org/10.1016/j.neulet.2005.05.003>
- Pepino, M. Y., Kuda, O., Samovski, D., & Abumrad, N. A. (2014). Structure-function of CD36 and importance of fatty acid signal transduction in fat metabolism. *Annual Review of Nutrition*, 34, 281–303. <https://doi.org/10.1146/annurev-nutr-071812-161220>
- Ricchi, M., Odoardi, M. R., Carulli, L., Anzivino, C., Ballestri, S., Pinetti, A., ... Loria, P. (2009). Differential effect of oleic and palmitic acid on lipid accumulation and apoptosis in cultured hepatocytes. *Journal of Gastroenterology and Hepatology*, 24, 830–840. <https://doi.org/10.1111/j.1440-1746.2008.05733.x>
- Richieri, G. V., & Kleinfeld, A. M. (1995). Unbound free fatty acid levels in human serum. *Journal of Lipid Research*, 36, 229–240.
- Rodriguez de Turco, E. B., Belayev, L., Liu, Y., Busto, R., Parkins, N., Bazan, N. G., & Ginsberg, M. D. (2002). Systemic fatty acid responses to transient focal cerebral ischemia: Influence of neuroprotectant therapy with human albumin. *Journal of Neurochemistry*, 83, 515–524. <https://doi.org/10.1046/j.1471-4159.2002.01121.x>
- Salvesen, G. S., & Rønsbo, M. (2002). Apoptosome: The seven-spoked death machine. *Developmental Cell*, 2, 256–257. [https://doi.org/10.1016/S1534-5807\(02\)00137-5](https://doi.org/10.1016/S1534-5807(02)00137-5)
- Sato, T., Machida, T., Takahashi, S., Murase, K., Kawano, Y., Hayashi, T., ... Niitsu, Y. (2008). Apoptosis supercedes necrosis in mitochondrial DNA-depleted Jurkat cells by cleavage of receptor-interacting protein and inhibition of lysosomal cathepsin. *The Journal of Immunology*, 181, 197–207. <https://doi.org/10.4049/jimmunol.181.1.197>
- Scheff, S. W., & Dhillon, H. S. (2004). Creatine-enhanced diet alters levels of lactate and free fatty acids after experimental brain injury. *Neurochemical Research*, 29, 469–479. <https://doi.org/10.1023/B:NERE.0000013753.22615.59>
- Schenkel, L. C., & Bakovic, M. (2014). Palmitic acid and oleic acid differentially regulate choline transporter-like 1 levels and glycerolipid

- metabolism in skeletal muscle cells. *Lipids*, 49, 731–744. <https://doi.org/10.1007/s11745-014-3925-4>
- Sergi, D., Morris, A. C., Kahn, D. E., McLean, F. H., Hay, E. A., Kubitz, P., ... Williams, L. M. (2018). Palmitic acid triggers inflammatory responses in N42 cultured hypothalamic cells partially via ceramide synthesis but not via TLR4. *Nutritional Neuroscience*, 23, 321–334.
- Shindo, R., Kakehashi, H., Okumura, K., Kumagai, Y., & Nakano, H. (2013). Critical contribution of oxidative stress to TNF $\alpha$ -induced necroptosis downstream of RIPK1 activation. *Biochemical and Biophysical Research Communications*, 436, 212–216.
- Silva, M. T. (2010). Secondary necrosis: The natural outcome of the complete apoptotic program. *FEBS Letters*, 584, 4491–4499. <https://doi.org/10.1016/j.febslet.2010.10.046>
- Smith, C. C., Davidson, S. M., Lim, S. Y., Simpkin, J. C., Hothersall, J. S., & Yellon, D. M. (2007). Necrostatin: A potentially novel cardioprotective agent? *Cardiovascular Drugs and Therapy*, 21, 227–233. <https://doi.org/10.1007/s10557-007-6035-1>
- Spector, A. A., John, K., & Fletcher, J. E. (1969). Binding of long-chain fatty acids to bovine serum albumin. *Journal of Lipid Research*, 10, 56–67.
- Spector, A. A., & Yorek, M. A. (1985). Membrane lipid composition and cellular function. *Journal of Lipid Research*, 26, 1015–1035.
- Stanger, B. Z., Leder, P., Lee, T. H., Kim, E., & Seed, B. (1995). RIP: A novel protein containing a death domain that interacts with Fas/APO-1 (CD95) in yeast and causes cell death. *Cell*, 81, 513–523. [https://doi.org/10.1016/0092-8674\(95\)90072-1](https://doi.org/10.1016/0092-8674(95)90072-1)
- Su, Z., Yang, Z., Xie, L., DeWitt, J. P., & Chen, Y. (2016). Cancer therapy in the necroptosis era. *Cell Death and Differentiation*, 23, 748–756. <https://doi.org/10.1038/cdd.2016.8>
- Sun, L., Xu, Y. W., Han, J., Liang, H., Wang, N., & Cheng, Y. (2015). 12/15-Lipoxygenase metabolites of arachidonic acid activate PPAR $\gamma$ : A possible neuroprotective effect in ischemic brain. *Journal of Lipid Research*, 56, 502–514.
- Tan, S. H., Shui, G., Zhou, J., Li, J. J., Bay, B. H., Wenk, M. R., & Shen, H. M. (2012). Induction of autophagy by palmitic acid via protein kinase C-mediated signaling pathway independent of mTOR (mammalian target of rapamycin). *Journal of Biological Chemistry*, 287, 14364–14376. <https://doi.org/10.1074/jbc.M111.294157>
- Tracey, T. J., Steyn, F. J., Wolvetang, E. J., & Ngo, S. T. (2018). Neuronal lipid metabolism: Multiple pathways driving functional outcomes in health and disease. *Frontiers in Molecular Neuroscience*, 11, 10. <https://doi.org/10.3389/fnmol.2018.00010>
- Tu, Q.-Q., Zheng, R.-Y., Li, J., Hu, L., Chang, Y.-X., Li, L., ... Wang, H.-Y. (2014). Palmitic acid induces autophagy in hepatocytes via JNK2 activation. *Acta Pharmacologica Sinica*, 35, 504–512. <https://doi.org/10.1038/aps.2013.170>
- Ulloth, J. E., Casiano, C. A., & De Leon, M. (2003). Palmitic and stearic fatty acids induce caspase-dependent and -independent cell death in nerve growth factor differentiated PC12 cells. *Journal of Neurochemistry*, 84, 655–668. <https://doi.org/10.1046/j.1471-4159.2003.01571.x>
- van der Vusse, G. J. (2009). Albumin as fatty acid transporter. *Drug Metabolism and Pharmacokinetics*, 24, 300–307. <https://doi.org/10.2133/dmpk.24.300>
- Vanlangenakker, N., Vanden Berghe, T., Bogaert, P., Laukens, B., Zobel, K., Deshayes, K., ... Bertrand, M. J. M. (2011). cIAP1 and TAK1 protect cells from TNF-induced necrosis by preventing RIP1/RIP3-dependent reactive oxygen species production. *Cell Death and Differentiation*, 18, 656–665. <https://doi.org/10.1038/cdd.2010.138>
- Vasquez, V., Krieg, M., Lockhead, D., & Goodman, M. B. (2014). Phospholipids that contain polyunsaturated fatty acids enhance neuronal cell mechanics and touch sensation. *Cell Reports*, 6, 70–80. <https://doi.org/10.1016/j.celrep.2013.12.012>
- Wang, Y., Wang, H., Tao, Y., Zhang, S., Wang, J., & Feng, X. (2014). Necroptosis inhibitor necrostatin-1 promotes cell protection and physiological function in traumatic spinal cord injury. *Neuroscience*, 266, 91–101. <https://doi.org/10.1016/j.neuroscience.2014.02.007>
- Wang, Z. J., Liang, C. L., Li, G. M., Yu, C. Y., & Yin, M. (2006). Neuroprotective effects of arachidonic acid against oxidative stress on rat hippocampal slices. *Chemico-Biological Interactions*, 163, 207–217. <https://doi.org/10.1016/j.cbi.2006.08.005>
- Wang, Z., Liu, D., Wang, F., Liu, S., Zhao, S., Ling, E. A., & Hao, A. (2012). Saturated fatty acids activate microglia via Toll-like receptor 4/NF- $\kappa$ B signalling. *British Journal of Nutrition*, 107, 229–241.
- Wassall, S. R., Leng, X., Canner, S. W., Pennington, E. R., Kinnun, J. J., Cavazos, A. T., ... Shaikh, S. R. (2018). Docosahexaenoic acid regulates the formation of lipid rafts: A unified view from experiment and simulation. *Biochimica et Biophysica Acta (BBA) - Biomembranes*, 1860, 1985–1993. <https://doi.org/10.1016/j.bbamem.2018.04.016>
- Wirawan, E., Vanden Berghe, T., Lippens, S., Agostinis, P., & Vandenabeele, P. (2012). Autophagy: For better or for worse. *Cell Research*, 22, 43–61. <https://doi.org/10.1038/cr.2011.152>
- Wu, X., Molinaro, C., Johnson, N., & Casiano, C. A. (2001). Secondary necrosis is a source of proteolytically modified forms of specific intracellular autoantigens: Implications for systemic autoimmunity. *Arthritis and Rheumatism*, 44, 2642–2652. [https://doi.org/10.1002/1529-0131\(200111\)44:11<2642::AID-ART444>3.0.CO;2-8](https://doi.org/10.1002/1529-0131(200111)44:11<2642::AID-ART444>3.0.CO;2-8)
- Xia, S., Lv, J., Gao, Q., Li, L., Chen, N., Wei, X., ... Xu, Z. (2015). Prenatal exposure to hypoxia induced Beclin 1 signaling-mediated renal autophagy and altered renal development in rat fetuses. *Reproductive Sciences*, 22, 156–164. <https://doi.org/10.1177/1933719114536474>
- Xu, S., Jay, A., Brunaldi, K., Huang, N., & Hamilton, J. A. (2013). CD36 enhances fatty acid uptake by increasing the rate of intracellular esterification but not transport across the plasma membrane. *Biochemistry*, 52, 7254–7261. <https://doi.org/10.1021/bi400914c>
- Yehuda, S., Rabinovitz, S., Carasso, R. L., & Mostofsky, D. I. (2002). The role of polyunsaturated fatty acids in restoring the aging neuronal membrane. *Neurobiology of Aging*, 23, 843–853. [https://doi.org/10.1016/S0197-4580\(02\)00074-X](https://doi.org/10.1016/S0197-4580(02)00074-X)
- Zhang, X., Yan, H., Yuan, Y., Gao, J., Shen, Z., Cheng, Y., ... Chen, Z. (2013). Cerebral ischemia-reperfusion-induced autophagy protects against neuronal injury by mitochondrial clearance. *Autophagy*, 9, 1321–1333. <https://doi.org/10.4161/auto.25132>
- Zhao, Y., Calon, F., Julien, C., Winkler, J. W., Petasis, N. A., Lukiw, W. J., & Bazan, N. G. (2011). Docosahexaenoic acid-derived neuroprotectin D1 induces neuronal survival via secretase- and PPAR $\gamma$ -mediated mechanisms in Alzheimer's disease models. *PLoS ONE*, 6, e15816.
- Zhou, W., & Yuan, J. (2014). Necroptosis in health and diseases. *Seminars in Cell and Developmental Biology*, 35, 14–23. <https://doi.org/10.1016/j.semcdb.2014.07.013>
- Zhu, S., Zhang, Y., Bai, G., & Li, H. (2011). Necrostatin-1 ameliorates symptoms in R6/2 transgenic mouse model of Huntington's disease. *Cell Death and Disease*, 2, e115. <https://doi.org/10.1038/cddis.2010.94>

**How to cite this article:** Montero ML, Liu J-W, Orozco J, Casiano CA, De León M. Docosahexaenoic acid protection against palmitic acid-induced lipotoxicity in NGF-differentiated PC12 cells involves enhancement of autophagy and inhibition of apoptosis and necroptosis. *J. Neurochem.* 2020;155:559–576. <https://doi.org/10.1111/jnc.15038>